

Civil Engineering Journal

(E-ISSN: 2476-3055; ISSN: 2676-6957)

Vol. 11, No. 09, September, 2025



Evaluating Rock Mass Quality and Critical Depth for Rockburst Hazard in Deep Mines

D. K. Takhanov ^{1, 2}, G. K. Sapinov ¹, M. Zh. Balpanova ^{1, 2*}, D. T. Ivadilinova ^{1*}, M. A. Zharaspayev ², Z. Zh. Abdrasheva ¹

¹Abylkas Saginov Karaganda Technical University, Karaganda 100027, Kazakhstan.

² Scientific and Technical Center for Industrial Safety LLP, Karaganda 100027, Kazakhstan.

Received 07 May 2025; Revised 11 August 2025; Accepted 20 August 2025; Published 01 September 2025

Abstract

This study investigates the geomechanical behavior of the rock mass at the Zhayssan mine in Kazakhstan, focusing on improving the safety of deep mining operations. The objective is to forecast the working strength of rock masses and assess the associated rockburst risks, especially given the limited existing data on the mechanical properties of the site's rocks. To achieve this, we conducted comprehensive laboratory tests to determine rock strength characteristics, brittleness, and elastic energy accumulation capacity. We analyzed these data using the Rock Quality Designation (RQD) indicator and constructed a simplified geomechanical model of the deposit. Our findings reveal that rock mass quality improves with depth, as indicated by higher RQD values and reduced fracturing intensity; however, this improvement coincides with an increased risk of dynamic rock pressure events, particularly beyond the analytically estimated critical depth of approximately 400 meters. The study's novelty lies in its integration of local testing data with comparative regional data, allowing for a more robust preliminary risk assessment despite limited local measurements. As promising directions, the paper suggests further laboratory and field research to refine methods for forecasting the strength and stability of mine workings.

Keywords: Rockburst Risk; Zhayssan Mine; Rock Quality Designation; Geochemical Model.

1. Introduction

Identifying the rockburst category of a rock mass at the design stage is crucial for promptly identifying risks and developing efficient safety measures. With insufficient information on geomechanical properties and increasing depth of operations, the probability of unpredictable geodynamic processes increases, which requires more accurate forecasting methods.

The interrelationship between the development depth and rock quality is the most important field of study in mining, especially during operations at great depths. Studies show that with increasing mining depth, the mechanical properties of the rock may improve due to increased overburden pressure, which increases the strength and stability of the rock. For instance, Lee et al. emphasize that the stress distribution characteristics in the surrounding rocks change significantly with depth, resulting in increased rock mass stability, which is crucial for safe mining operations [1]. This stability is also supported by the findings of Wu et al., who discuss how the deformation of the surrounding rocks is affected by high geo-stress conditions that occur with increasing mining depth, indicating a complex interaction between geologic factors and mining methods [2]. Moreover, as Zhang et al. [3] noted, the mechanical behavior of

^{*} Corresponding author: balpanova86@mail.ru; dina.ivadilinova@gmail.com





© 2025 by the authors. Licensee C.E.J, Tehran, Iran. This article is an open access article distributed under the terms and conditions of the Creative Commons Attribution (CC-BY) license (http://creativecommons.org/licenses/by/4.0/).

rocks at greater depths tends to shift from brittle to ductile characteristics. This transformation can improve rock quality as deeper rock masses are exposed to various influences that can enhance their structural integrity. However, it is essential to recognize that while some aspects of rock quality may improve, problems such as rock falls and dynamic disasters also become more pronounced with increasing depth, requiring enhanced monitoring and management strategies [3, 4]. Using reliable walling technologies is crucial for maintaining rock stability in deep mining operations. Kahn emphasizes that as the depth of mining operations increases, the *in-situ* stresses also increase significantly, making it difficult to reinforce roads and other underground structures [5]. Developing durable fastening elements has addressed these challenges; they enable better control, accommodate larger deformations, and enhance the overall safety of mining operations [6]. In addition, using numerical modelling methods, as described by Gazdali et al. [7], provides valuable information on the stability of mine workings in low-quality rocks, further illustrating the importance of adapting mining methods to the geological conditions encountered at depth. While deeper mining can improve rock quality through increased stability and strength, it also presents significant challenges that require careful management and innovative engineering solutions. The relationship between depth, rock mechanics, and mining methods is critical in optimizing mining processes and ensuring mining safety.

Although recent studies significantly advanced the understanding of rockburst mechanisms and deep rock mass behavior [1–7], several limitations remain when applying these methods to specific field conditions, such as at the Zhayssan mine. For instance, Sun et al. [8] and Wang et al. [9] proposed robust data-driven models for rockburst forecasting; however, their effectiveness strongly depends on large, labelled datasets, which are unavailable for new or remote mines. Zhou et al. [10] and Zeitinova et al. [11] emphasized stress-strain evolution with depth but lacked consideration for metasomatic alterations or brittle-ductile transitions in granitic rock masses. Field-based insights from Zholmagambetov et al. [12], Abdiev et al. [13], and Rojas Perez et al. [14] highlighted practical challenges in deep mines, yet these case studies focused on coal or polymetallic deposits with differing geological contexts. Hekmatnejad et al. [15] presented empirical criteria for burst-prone conditions but did not account for geological heterogeneity and stress anisotropy in brittle granitoids.

Thus, despite substantial progress, there is a noticeable gap in geomechanical modeling and risk forecasting approaches tailored to deep, brittle, metasomatically altered granitoid formations under thrust-fault tectonic regimes. The Zhayssan mine represents a case where in situ stress measurements are limited, laboratory data is scarce, and complex tectonic conditions prevail. Accordingly, this study aims to address these limitations by integrating laboratory testing, field analogues, and a simplified geomechanical model based on the Rock Quality Designation (RQD) index to forecast working strength and evaluate rockburst risks with depth under local geological constraints.

The Zhayssan mine is in the southeastern part of Kazakhstan and is operated by Zhanashyr Project LLP. Despite insufficient knowledge of the rock's mechanical properties during the construction phase of the underground mine, legislation requires assessing the rock mass for rockburst. Additionally, one of the reasons for this study is the unexpected geodynamic phenomena that occurred at the Shatyrkul underground mine, which is located nearby, approximately 25 km from the Zhayssan mine.

According to the regulations of the Republic of Kazakhstan, rock deposits and rock masses, or parts thereof, that contain rocks with high elastic properties and are capable of brittle fracture under load are considered to have rockburst potential. Rockburst zones also include areas with rock bursts, intense flaw formation, or tremors, and rockbursts at a neighboring mine within the same ore body and under similar geological conditions. The nature of damage in the mine workings at Shatyrkul mine and research confirm that the rocks at this mine are prone to rockbursts; this raises the question: what depths should be considered as the ones having rockburst potential at Zhayssan mine?

The Zhayssan ore field consists of granitoid intrusions: granodiorites and biotite-granites of the Upper Ordovician (450–480 Mya). Contacts between the granodiorites and granites are intrusive and irregular. Biotite-granites form an endocontact rim of granodiorites. All ore zones of the deposit are confined to the contacts of granites and granodiorites. Diabase dikes in Zhayssan are more developed than in Shatyrkul. The ore zones occur roughly parallel to each other.

The characteristic features of the deposit are:

- The very frequent coincidence of ore-bearing tectonic zones along strike and dip with diorite dykes and diabaz porphyrites
- The presence of a "jacket" of hydrothermally altered rocks with a thickness of tens of meters around the ore bodies; at the contacts of thick ore bodies, hydrothermal metasomatosis of granitoids leads to the formation of sericitized rocks (up to clay-like) with reduced strength, prone to soaking when watered.

No *in situ* measurements of natural stresses have been made at the Zhayssan mine. They were initially assessed according to the 2016 database of the international World Stress Map (WSM) project. In southern Kazakhstan (Figure 1), the natural stress condition of the rock mass is characterized by the tectonic mode of Thrust Faulting (TF) (Figure 2).



Figure 1. Crustal stress in southern Kazakhstan and Kyrgyzstan on the WSM (coordinates: N43°32' E74°25')

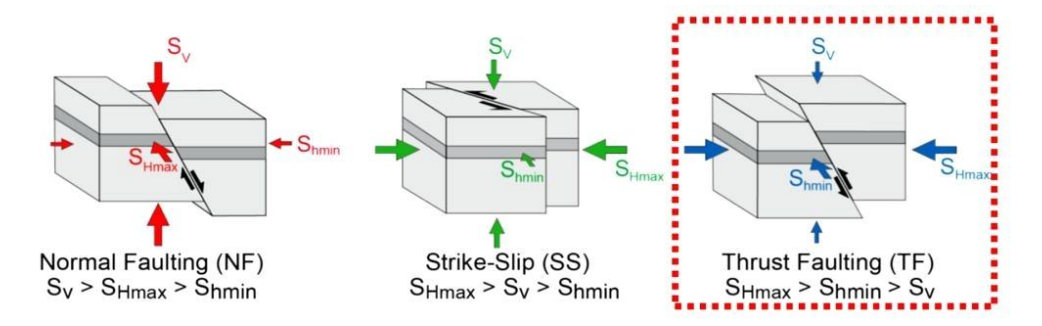


Figure 2. Three main tectonic regimes of the natural condition of the rock massive, differing in the action directions of the main stresses

The tectonic mode of Thrust Faulting TF means the following ratio of the main natural stresses [16-18]:

- Maximum by value is horizontal tectonic stresses $\sigma_l = SHmax$; the action direction in the plane is shown by hachure in the WSM
- Horizontal stresses $\sigma_2 = SHmin$, acting perpendicular to the maximum ones, are intermediate in value
- Vertical gravitational stresses from the weight pressure of the rock strata are minimal in value $\sigma_3 = SV = \gamma H$:

 $SHmax > Shmin > \gamma H$.

According to the WSM 2016 (Figure 1), in southern Kazakhstan, horizontal tectonic stresses that are maximum in their value $\sigma 1$ act in a sub-meridional direction close to the N-S direction.

Tectonophysics methods have obtained similar results in the neighbouring Kyrgyzstan region [19]. The maximum tectonic (horizontal) stresses in the Shatyrkul and Zhayssan mines act in the north-eastern direction, approximately along the strike of the ore zones.

Figure 3 shows the results of in situ measurements of natural stresses at mines in Kyrgyzstan [19]. Their processing resulted in the following estimates of natural horizontal stresses: $\sigma_1 = 3.1 \text{ yH}$; $\sigma_2 = 1.9 \text{ yH}$. Vertical stresses from the gravitational pressure of the rock strata are minimal $\sigma_3 = yH$.

These results show that at Shatyrkul and Zhayssan mines, the maximum tectonic (horizontal) stresses along the strike of the ore zones σ_l may exceed the vertical pressure of the overlying strata γH thrice. At depths H = 500-600 m provided by the mining projects, high tectonic stresses can create rockburst situations in strong, elastic, brittle granitoids without any change caused by hydrothermal metasomatosis.

To clarify the predicted and calculated geomechanical situation in the past mine workings at Shatyrkul and Zhayssan mines, it is necessary to conduct research and development work to determine their rockburst potential.

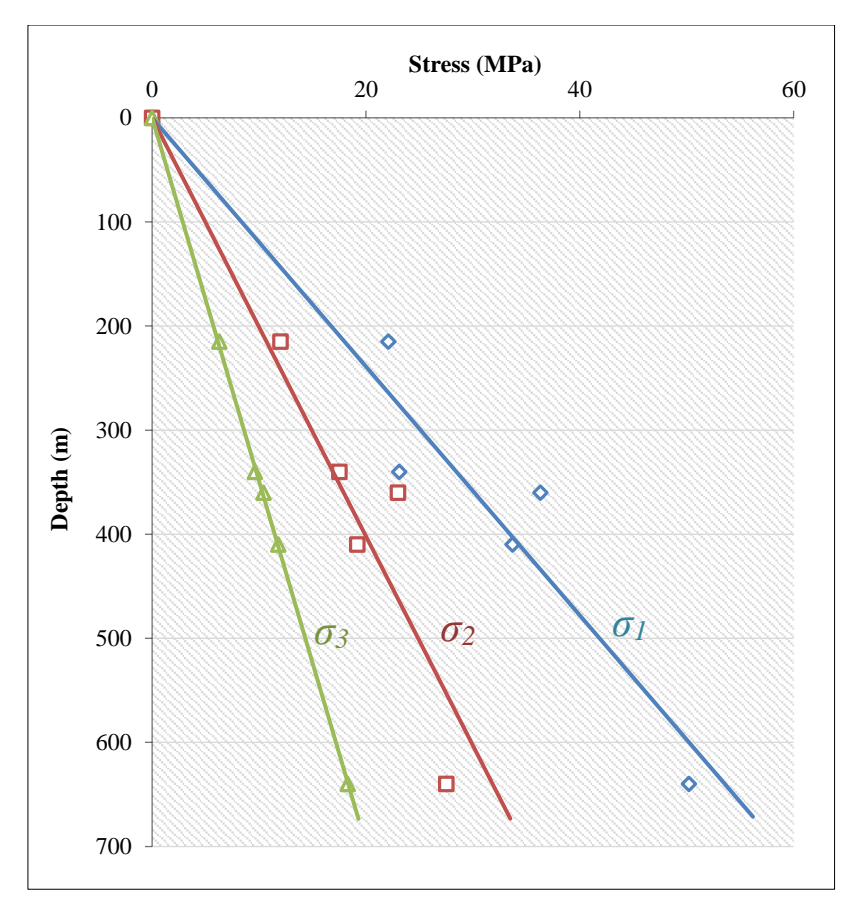


Figure 3. Natural stresses at Kyrgyzstan mines (Turangli, Mirgalimsay, Kurusay, Khaidarkan, Kadamzhay) with tectonic mode of thrust faulting

2. Research Methodology

The research applied complex geomechanical methods, including the study of geological features of the deposit, assessment of the natural stress condition of the rock mass based on regional tectonophysical data and in-situ stress measurements, laboratory studies of mechanical properties of rocks considering the influence of metasomatic processes, and detailed analysis of the structure and fracturing of the rock mass according to the RQD indicator. Based on these data, a three-dimensional geomechanical model of the rock mass was constructed using the Kriging method. The stability of mine workings was forecasted, including a kinematic analysis of possible rock inrushes. The rockburst was assessed by analyzing the brittleness coefficient and impact rockburst potential. Based on the results, recommendations on managing rock pressure and designing effective measures to ensure the stability and safety of mine workings were formed.

2.1. Mechanical Properties of Rocks

The mining project for the Zhayssan deposit [20] uses the coefficients of the Protodyakonov scale of hardness: for sulfide ores f = 8-10; for oxidized ores f = 8-9; for granites f = 9-11 that had been preliminarily estimated at the stage of geological exploration. i.e., the host rocks are stronger than the ore. i.e., the amount of research conducted is unknown, and this conclusion requires verification. Kazakhmys has a history of misleading data on the ore/rock strength used in projects, resulting in adverse consequences [21-23].

The rock properties at the Zhayssan deposit are not sufficiently studied: 100 samples of granite, granodiorite, and diabaz underwent compression and extension tests. These samples were collected from 47 exploration boreholes, covering depth intervals from the surface to approximately 540 meters. Although the number of specimens per lithotype and depth range is limited (typically 4–7 per test), statistical methods such as t-tests and histogram analysis were applied to detect heterogeneity. To increase the confidence of extrapolated trends, the results were further compared and validated using analogous datasets from the geologically similar Shatyrkul mine. Although each test type involved only 4–7 samples, the use of statistical methods and analogue site comparison helped mitigate this limitation. Studying the reduction in rock strength within the metasomatosis zone is also necessary. The summarized results of rock testing for the Zhayssan deposit are given in Table 1.

Table 1. Zhayssan Deposit Rock Properties

Sample No.	Rocks	True density (g/cm³)	Bulk density (g/cm³)	Elastic module, (10 ⁴ MPa)	Poisson's ratio	Compression strength (MPa)				Number of	Tensile	Factors	
						Number of samples	In dry state	Number of samples	In water- saturated state	-Number of samples	strength (MPa)	Softening	Brittleness
1	Granodiorite	2.70	2.68	4.5	0.14	7	99	7	87	7	7.7	0.88	13
2	Diabaz	2.77	2.76	4.6	0.14	6	77	5	64	4	7.6	0.83	10
3	Granite	2.65	2.63	4.2	0.14	5	87	6	68	4	8.6	0.78	10
	Mean Value	2.71	2.69	4.5	0.14	-	86	-	74	-	8.0	0.86	11

Under compression, the average strength of Zhayssan granitoids ranges within 80-100 MPa. According to the international classification ISRM, these are strong rocks (strong) R4 [24, 25]. They do not soften much when watered. These are rather rigid rocks with a high elastic modulus. According to the compression and tensile strengths ratio, they are brittle rocks. This set of mechanical properties makes them prone to rockbursts at high mountain pressures.

In this forecast, the lack of actual data on Zhayssan is compensated by the data from the Shatyrkul deposit. This nearest deposit is like Zhayssan in terms of genesis (hydrothermal), lithology (granitoids), structural architecture (steeply dipping ore zones of medium and low thickness), and natural stress condition of the rock mass (tectonic mode of thrust faulting with a predominance of tectonic stresses over gravitational pressure).

The experience of the Shatyrkul mine shows that it is necessary to distinguish between primary rocks unaffected by hydrothermal metasomatism (fresh) and metasomatically altered rocks (altered). During the hydrothermal transformation of granitoids, plagioclases, feldspars, and other coloured minerals transform into sericite and chlorite. Metasomatically altered granitoids lose strength, elasticity, and brittleness (up to a clay-like state) and become prone to soaking when watered. The laboratory data showed that water saturation has a noticeable softening effect, particularly in altered rocks. Compared to dry states, the UCS of altered granitoids dropped by more than 20%, highlighting their increased vulnerability in the presence of groundwater. Although groundwater flow modeling was not part of this study, the results underscore the importance of integrating hydrogeological assessments in future research, especially when altered zones intersect with deep-level workings. Figure 4 shows the UCS compressive strength histogram for all types of magmatic rocks without dividing them into fresh and altered. The UCS pooled statistics comprise test results for 104 samples.

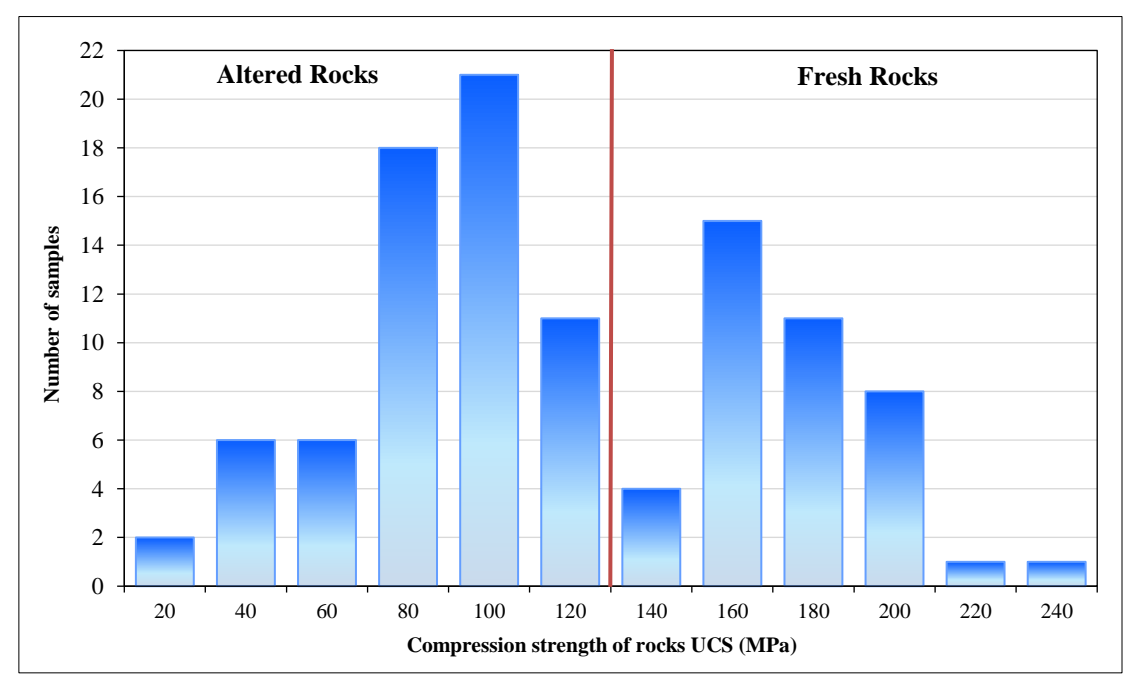


Figure 4. Compression strength distribution for all rock types of the Shatyrkul deposit

The UCS strength statistic has a bimodal distribution (with two maxima); this indicates that the statistics are heterogeneous, i.e., it comprises two types of rock with different properties. These are strong fresh rocks and metasomatically altered rocks of medium strength. The average strength of all rock types is UCS = 110 MPa with a standard deviation Sd = 50 MPa. The coefficient of strength variation that equals V = 50/110 = 56% is almost 2 times higher than the acceptable V = 30-35%. This fact confirms the heterogeneity of the sample.

To compare the average strengths of Shatyrkul and Zhayssan rocks, the Student's *t*-test [26] (with a significance level of 1%) was used, and it confirmed statistically significant differences between the samples (Table 2); this means that the average strength of Zhayssan rocks is less than in Shatyrkul.

Table 2. Comparison of rock strengths at Zhayssan and Shatyrkul Mines

	Shatyrkul (1)	Zhayssan (2)			
Number of tests n	104	18			
Mean strength UCS, MPa	110	87			
Standard deviation Sd, MPa	50	29			
Student's t-test T	$T = \frac{USC_1 - USC_2}{\sqrt{\frac{Sd_1^2}{n_1} + \frac{Sd_2^2}{n_2}}}$ $T = 2.81$				
Number of degrees of freedom	120				
Significance level α	0.01				
Critical Student's t-criterion	$t_{\alpha}=2.62$				
Comparison result	$T > t_{\alpha}$				
Conclusion:	Mean values of strength for the samples (1) and (2) have a statistically significant difference				

At the Shatyrkul deposit, the conventional boundary between the two rock types (fresh and metasomatically altered granites) can be taken by their strength UCS = 120 MPa. If we divide the raw statistics into two populations, we can estimate the strengths of fresh and metasomatically altered rocks. A comparison of the histograms of the two samples is shown in Figure 5 and Table 3.

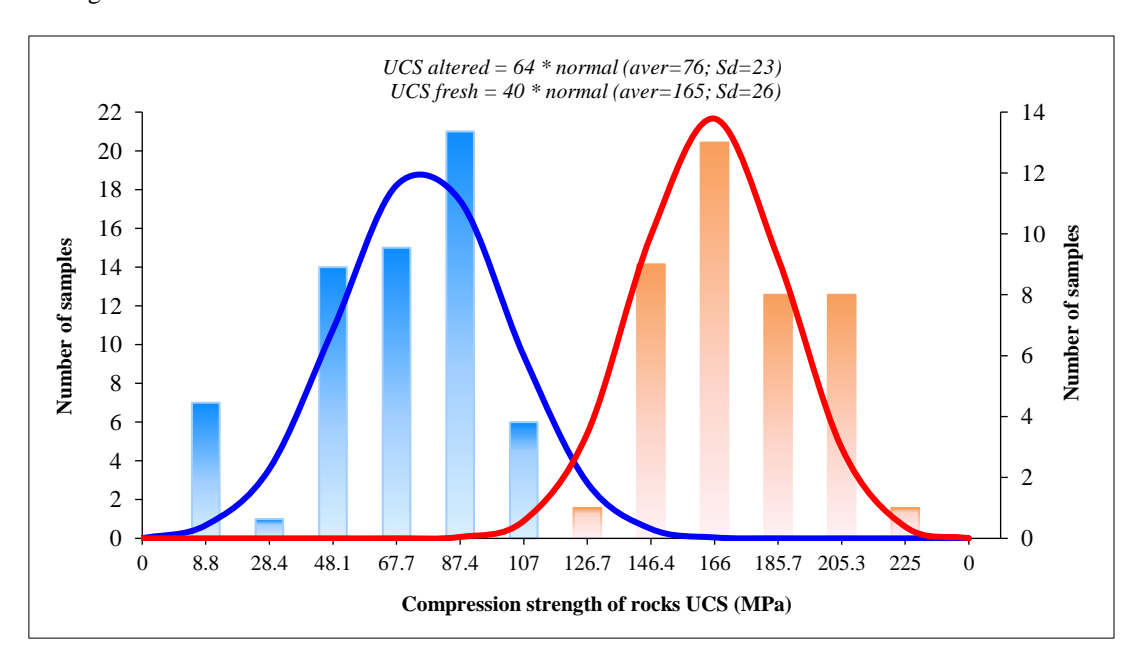


Figure 5. Difference in strengths of metasomatically altered (blue) and fresh rocks (red) at the Shatyrkul deposit

Table 3. Comparison of properties of hydrothermally altered and fresh rocks at Shatyrkul deposit

Indicators of rock strength for	Rocks				
uniaxial compression UCS	Altered	Fresh			
Number of tests	64	40			
Mean strength, MPa	76	165			
Standard deviation, MPa	26	23			
Variation factor	34%	14%			
Rigidness Rigidness category acc. To PTE	7 Mean Rigidness	16 Rigid Enough			

Around the ore zones in the "jacket" of metasomatically altered rocks, their strength is 2.2 times lower than that of the source granitoids. According to the PTE classification, the strengths of the two rock types are grouped into two categories. After splitting the original heterogeneous statistic into two samples, the variation coefficients decreased to an acceptable level; this means that the physically clear differences in the two rock types (fresh & altered) are confirmed statistically.

Based on the experience of the Shatyrkul mine, the main manifestations of rock pressure are observed during excavation in metasomatites, which have reduced strength and increased fracturing. To minimize the manifestations of the rock pressure, based on the accumulated practical experience, mining measures are used to protect mine workings at the design stage-capital and preparatory workings are in fresh rocks with higher strength and lower fracturing.

2.2. Rock Mass Fracturing

The expected fracture systems forecast will be based on the study results of a deposit like Shatyrkul. The polar graph of the rock mass fracturing based on the results of surveying in the Dips program is shown in Figure 6.



Figure 6. Fracture systems at Shatyrkul Mine

Based on the orientations of 702 measured fractures, three systems are identified in the graph. Their average dip angles (Dip) and dip azimuths (Dip Direction) in the table in Figure 7 are highlighted in red. The same graph shows the blue lines of the mean strike (Figure 6) and the dip of the ore zone. Relative to these, the major fracture systems are oriented as follows:

The first system (1m) consists of steeply dipping ($Dip = 75-90^{\circ}$) fractures consistent with the strike and dip of the ore zone; generally, these are the most common fractures with great length;

the second system (2m) consists of inclined (Dip = $40-55^{\circ}$) fractures consistent with the strike but with reverse (concerning the ore zone) dip; this system can be called longitudinally secant;

The third system (3m) consists of steep dipping (Dip = 65-90) fractures that cut across the strike of the ore zone at an angle close to 90° ; this system can be called a cross-secant system.

The DFN (Discrete Fracture Network) module constructs a fracture network in the dip-oriented cross-section. This plane displays the first and second fracture systems with average dip angles of 81° and 53° (Figure 7). These fracture systems cause kinematic instability of entries that run along the strike of the ore zone. Kinematic instability is expressed in intensive rock block inrushes from the sides and roof of the entries along steeply falling fractures under their weight. It is difficult, expensive, and unsafe to prevent such rock inrushes by bracing.

Similar fracture systems (at least the major ones) should be expected at Zhayssan Mine (Figure 8). Therefore, the problems of supporting entries along the strike of the ore zones will be similar. Similar measures shall be taken to ensure the stability of entries.

To forecast the working stability and justify parameters of mining measures to protect the entries, the mine geomechanics engineer shall continuously map the rock mass fracturing during the sinking process. It is necessary to measure the elements of fracture occurrence (dip angle and azimuth using a mining compass), lengths, distances between fractures in the systems, degree of their roughness, presence of filler, and signs of weathering.

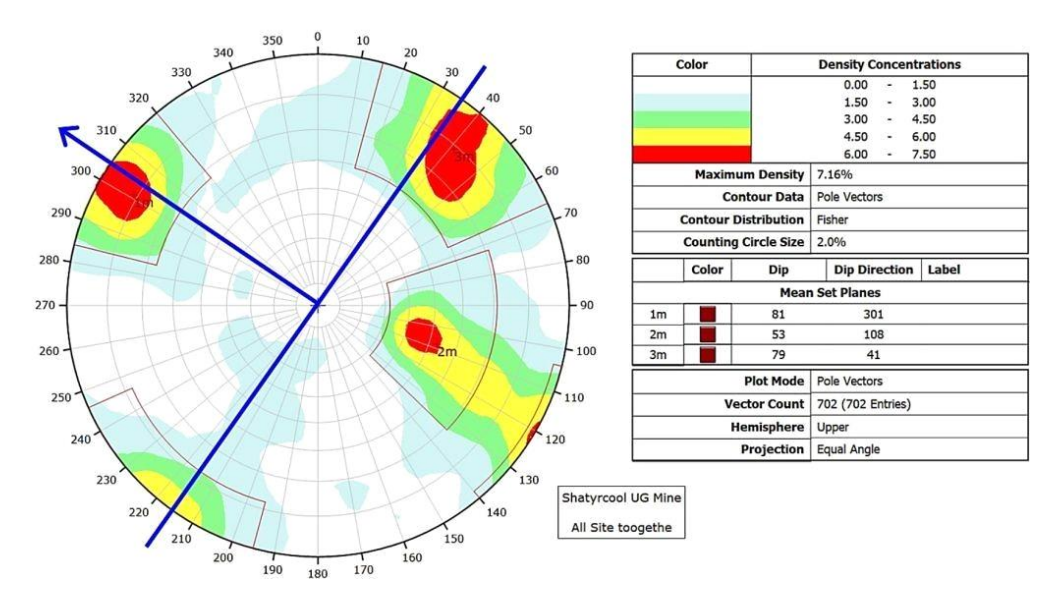


Figure 7. Inrushes of rock mass blocks in entries along the strike along steeply falling fractures under their weight

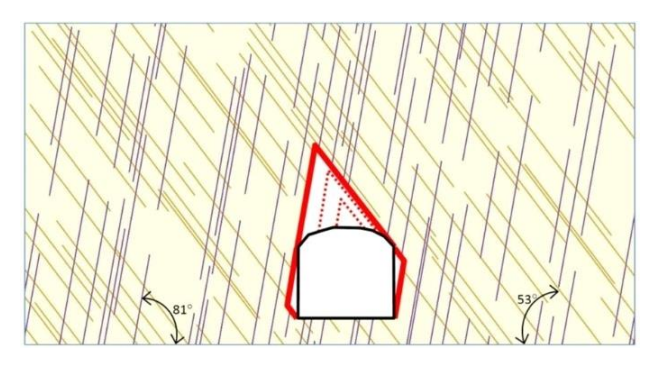


Figure 8. Rock mass fracturing in a trench side of the transportation slope No. 2. fracture systems: 1 m - according to the dip of the rock strata; 2 m - according to the secants; 3 m - cross-sectional

2.3. RQD Indicator

During the additional exploration of the Zhayssan deposit, the geological description of the core identified the geomechanical indicator of the rock mass fracturing - RQD (Rock Quality Designation). This indicator is used in almost all modern methods of geomechanical calculations. It is determined according to core intervals, typically the length of the drilling flight. A characteristic view of the core in Zhayssan is shown in Figure 9.

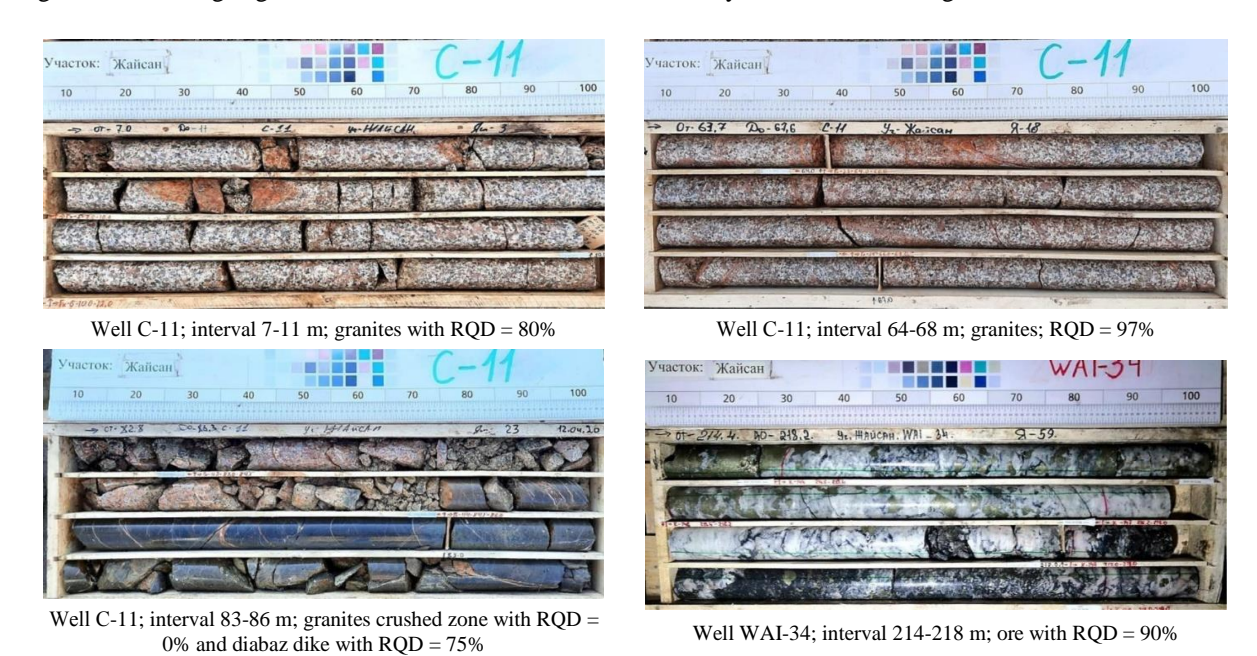


Figure 9. Appearance of the main rock types core of the Zhayssan deposit

Five thousand four hundred and nine core intervals of 1-3 m length were described in 47 wells with index C (11 pcs.), WAI (16 pcs.), ZH...Tech (20 pcs.) with diameter HQ. The RQD statistics are summarised in Figure 10.

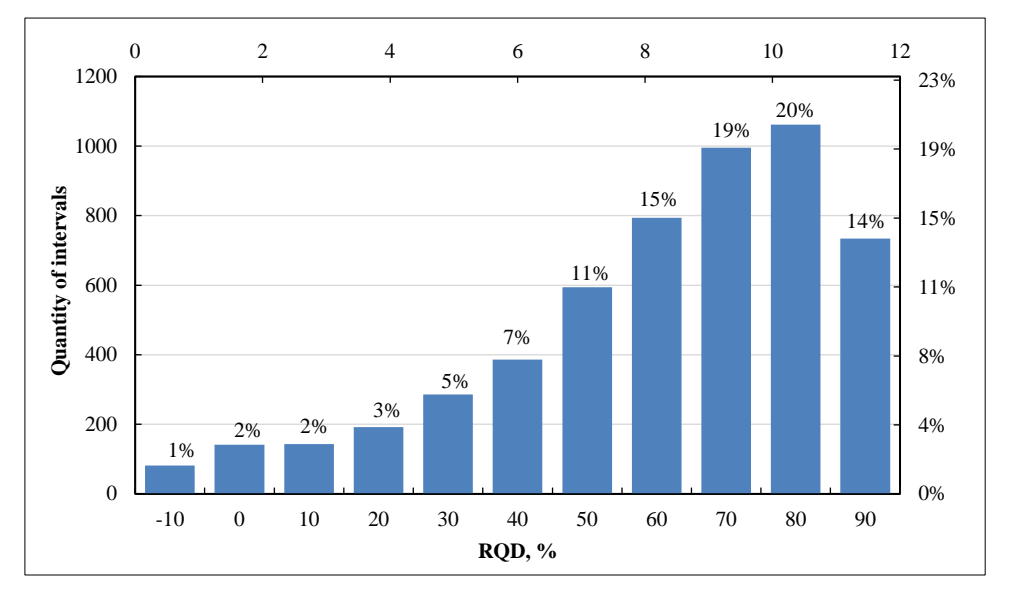


Figure 10. RQD histogram for Zhayssan deposit

The distribution has the appearance of an inverse logarithmically normal distribution. It is asymmetrical, with high values dominating (RQD = 100-60%); their share is 68%. The "tail" of low values fades within the range of RQD = 50-0%. This type of histogram is characteristic of strong, weakly fractured rocks with relatively thin zones of tectonic disturbances and low RQD values.

When the distribution is asymmetric, the mean value of the index underestimates the rock mass quality. A more objective value is the modal (most common) value. At Zhayssan: mean RQD = 67%, mode RQD = 85%. The modal value of RQD was used as a boundary condition to create a block geomechanical model of the deposit. With the depth growth, the fracturing of the rock mass slightly decreases as the average RQD values slightly increase (Figure 11); this means that the greatest problems with working stability can be observed at the uppermost horizons.

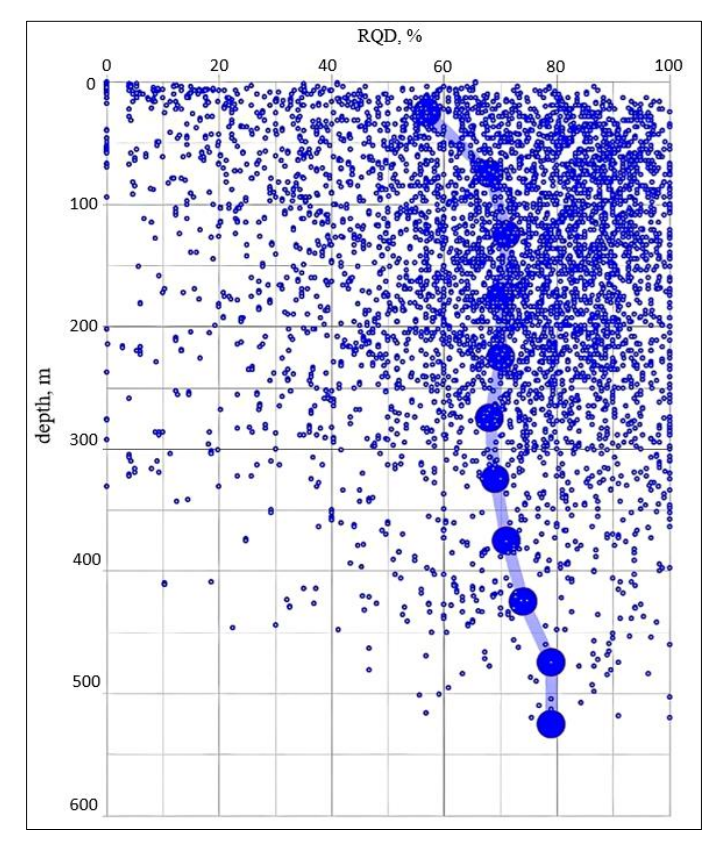


Figure 11. RQD changes depending on the depth at the Zhayssan deposit

This observation is important because it contradicts the intuitive assumption that greater depths always pose higher risk. It highlights that shallow levels require more attention to support design due to weaker, more fractured rock. Operational strategies should reflect this by reinforcing early development levels accordingly.

2.4. Block Geomechanical Model of the Rock Mass at Zhayssan Deposit

2.4.1. Input Data

The geological structure of the deposit was studied during its detailed exploration. It is shown on plans of horizons 1040, 970, 870, 770, 670, 570, and 470 m and geologic sections 7, 9, 11, 13, and 15. This 2D graphical information was used to create a three-dimensional model of the deposit in the Leapfrog program by fixation on the coordinates and marks.

The results of the geomechanical description of the core of 47 wells drilled in 2018-2020 were used to fill the block geomechanical model for (a) additional exploration, b) stock certifications, and c) process sampling for ore processing.

One geomechanical parameter of RQD was determined during the core description. Therefore, at the present stage of the deposit development, the geomechanical model can only be simplified due to insufficient knowledge of the rocks' mechanical properties and lack of data on rock mass fracturing. The coloring of the exploration well shafts in Figure 12 displays the RQD values. Green-light blue-blue colors = high RQD values in weakly fractured rock masses. Yellow-orange-red = low RQD values in highly fractured rock masses, crushed zones, and tectonic faults.

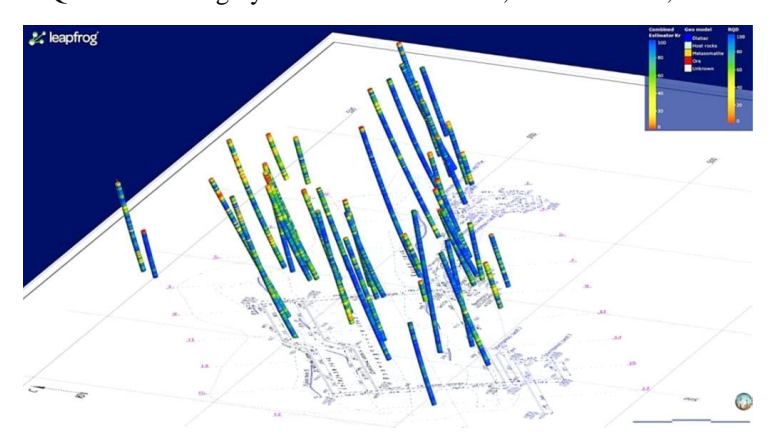


Figure 12. Geomechanical database on exploration well cores

2.4.2. Geological Model of the Deposit

The geological hood of the created 3D model has the following dimensions: West-East = 2200 m, North-South = 1400 m, and by depth = 520 m. It should be noted that the rock mass is more or less studied to the mark of 770 m. The general appearance of the geologic model of the Zhayssan deposit is shown in Figure 13. It uses the following rock mass types:

- Fresh granites and granodiorites represent host rocks = the host rocks;
- Metasomatite = metasomatically altered host rocks (altered);
- Diabaz = diabaz dikes;
- Ore = ore bodies.

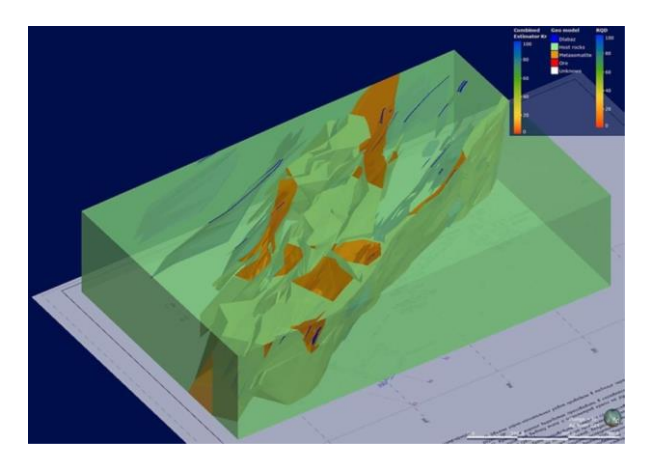


Figure 13. General view of the geological model of the Zhayssan deposit

The colouring of rock types is shown in Figure 13. For example, A section of the geologic model along Line 11-11 is shown in Figure 14.

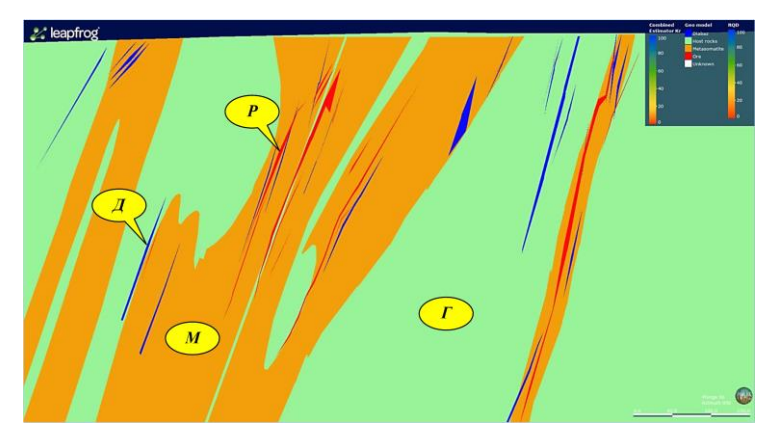


Figure 14. Section of the geologic model along lines 11-11: P – ore bodies; \mathcal{A} – diabaz dikes; M – metasomatically altered rocks (altered); Γ – fresh granitoids (fresh)

2.4.3. Geomechanical Model of the Deposit

The current stage of the geomechanical study of the Zhayssan deposit can be called the initial stage (Scoping Study). Therefore, due to the lack of input data on ore and rock properties, fracturing, and natural stress condition of the rock mass, it is not yet possible to build a complete block model of the rock mass filled with such important indicators as:

- Benyavskiy RMR (Rock Mass Rating);
- Barton rock mass quality index Q (Quality Index);
- GSI (Geological Strength Index);
- Strength of a fractured rock mass.

So far, only a simplified geomechanical model of the deposit can be built. It utilizes the RQD indicator since it determines the fractured rock mass GSI (Geological Strength Index) [27]:

$$GSI = \frac{52J_r/J_a}{1+(1+J_r/J_a)} + \frac{RQD}{2} \tag{1}$$

where Jr, Ja - Barton's indicators characterize fracture roughness and their filling or degree of weathering [28].

GSI is used to calculate the strength of a fractured rock mass. For this purpose, the generalized Hooke-Brown criterion is used [27]:

$$\sigma_1 = \sigma_3 + UCS \cdot \left(m_b \frac{\sigma_3}{UCS} + s \right)^a \tag{2}$$

Parameters of the strength criterion for a fractured rock mass are; UCS: unconfined rock strength of rocks in undisturbed samples; and m_b : Hooke-Brown parameter depending on the rock type (the equivalent of the angle of internal friction in the Coulomb-Mohr strength criterion):

$$m_b = m_i \cdot exp\left(\frac{GSI - 100}{28 - 14D}\right) \tag{3}$$

where; m_i – parameter determined from the rock strength certificate based on triaxial compression tests;

$$s = exp\left(\frac{GSI - 100}{9 - 3D}\right) \tag{4}$$

where; s: Hooke-Brown parameter (the equivalent of the cohesion in the Coulomb-Mohr strength criterion), and D – parameter considers the strength reduction due to rock mass damage by blasting.

The generalized Hooke-Brown criterion for the fractured rock mass strength defines the limits for the maximum major acting stresses σ_1 in the triaxial stress state (under the action of the minimum major stresses σ_3). This criterion calculates the safety factor in the numerical modelling of geomechanical situations. Also, RQD is the basis for calculating the Barton rock mass quality index Q [28, 29].

2.4.4. Simplified Geomechanical Model of Zhayssan Deposit

The input data for the model construction are described in section 2.4.1. To populate the block model, RQD values were interpolated using the Kriging method in 3 passes [30]. Different variogram parameters were used for each of them (Table 4); this allowed for achieving a more accurate RQD interpolation in areas where the density of the input

data is higher. The first two passes used a variable orientation of the search ellipsoid created based on the main fault planes on the object. For the third pass, the global trend set by the average dip values of the two main fault zones was used: $Dip = 69.4^{\circ}$; $Dip Direction (Azimuth) = 327^{\circ}$. The resulting passes are combined in the block model.

General		Ellipsoid Ranges				Ellipsoid Directio	Variable Orientedien		
Name Values		Maximum	Intermediate	Minimum	Dip	Dip Azimuth	Pitch	Variable Orientation	
Kr, RQD 1 pass	RQD	373	224	74.5				Variable Orientation Faults	
Kr, RQD 2 pass	RQD	700	500	250				Variable Orientation Faults	
Kr. ROD 3 pass	ROD	800	600	400	69.4	327	1.03		

Table 4. Parameters of RQD Search Ellipsoids by Kriging Method

At the outer borders of the interpolation volume, a modal value of RQD = 85% was applied. Visual inspection of the realism of the interpolation showed no contradictions with the input data. The interpolated RQD values fill the block model of the rock mass with block sizes of $10\times10\times10$ m. An axonometric view of the block model of the RQD array is depicted in Figure 15.

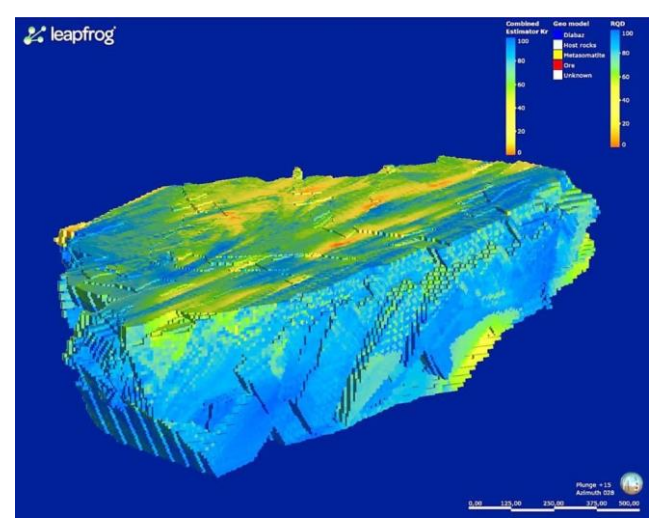


Figure 15. 3D Block model of rock mass RQD for Zhayssan deposit

At the Zhayssan mine, the current density of accumulated geomechanical data for horizon 970 m is depicted in Figure 16.

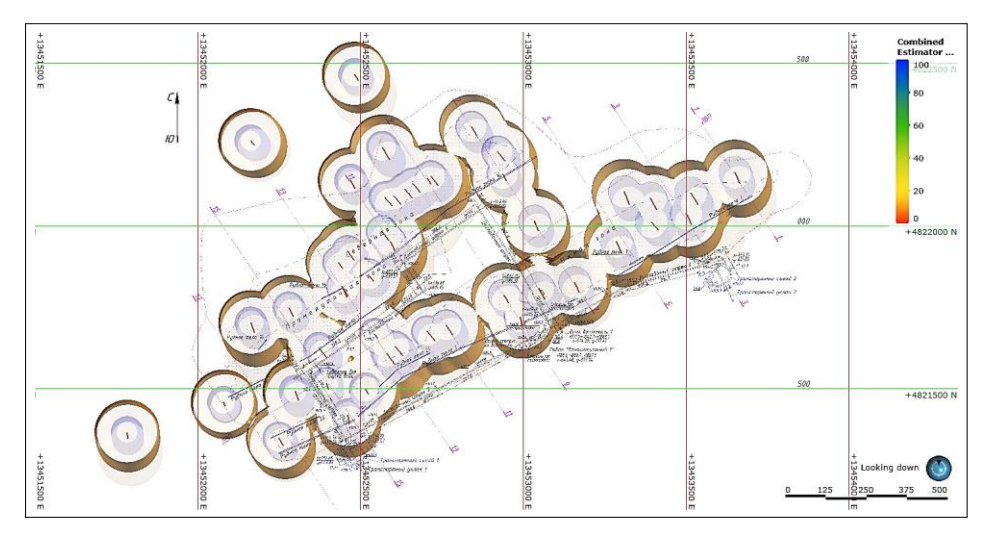


Figure 16. Density of GDD geomechanical data for Horizon 970 m: blue cylinders with a radius of 50 m around the wells; olive ones with a 100 m radius

Cross sections showing the RQD distribution for the mark of 970 m were plotted in the Leapfrog program (Figure 17) and in sections 11-11 (Figure 18). In these figures, the light blue-blue fill indicates high RQD values in weakly disturbed rock masses. It can be assumed that such rock masses will be stable. Green-yellow-orange shading indicates low RQD values in moderately to highly disturbed rock masses, the stability category of which would be downgraded to medium and unstable.

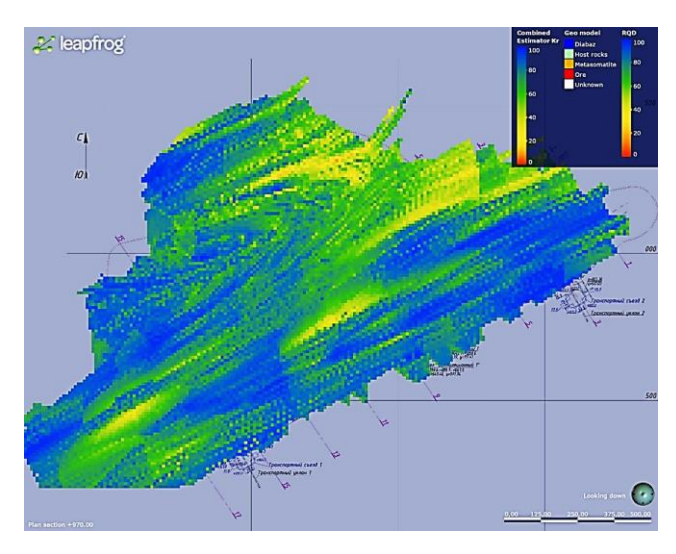


Figure 17. RQD distribution for horizon 970 m

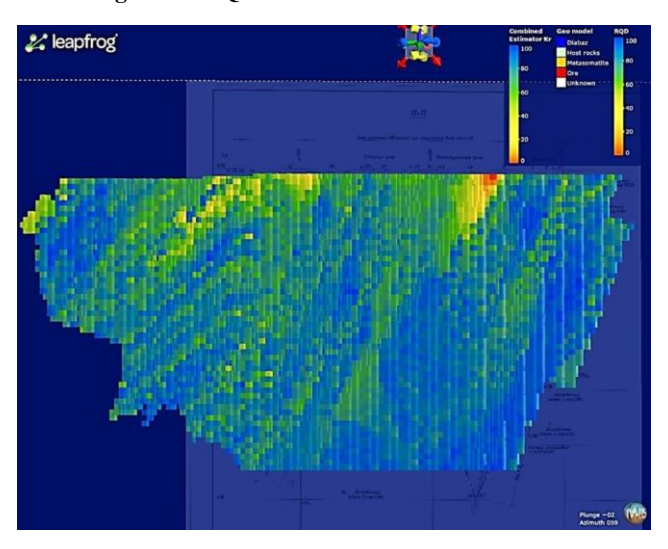


Figure 18. RQD distribution in sections 11-11

To establish the pattern of RQD variation with depth from the block geomechanical model, horizontal slices (Swath) were made in 10 m depth increments. The average RQD value at a given depth was calculated in each slice. Figure 19 shows its variation with depth. The black line shows the average values by wells; the red line shows interpolated values in the model.

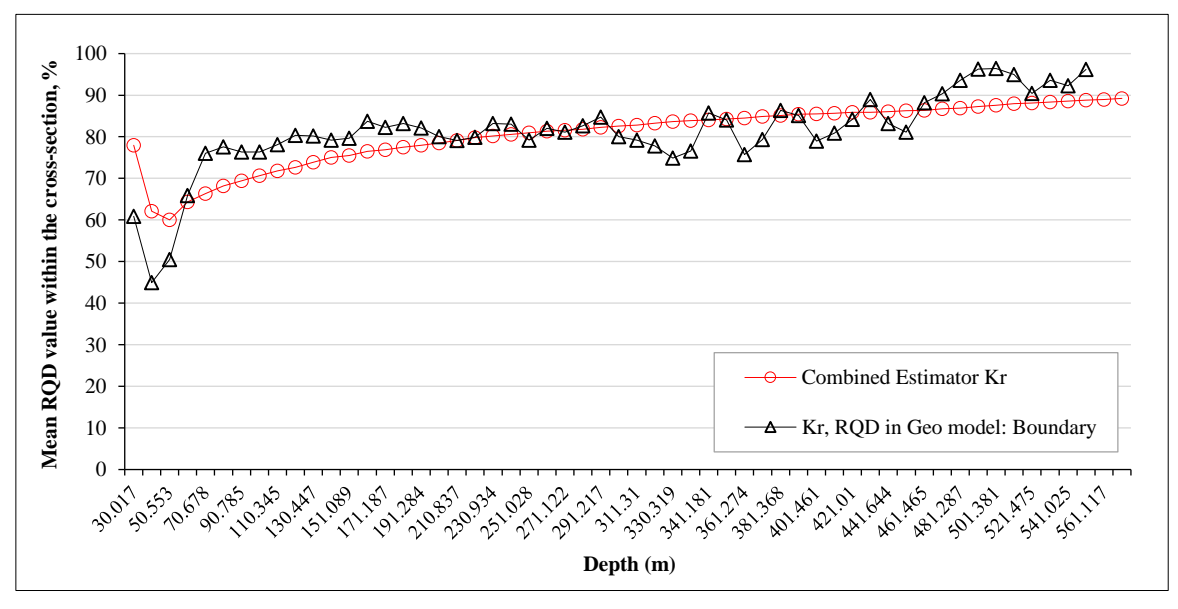


Figure 19. RQD Growth with depth

2.5. Theoretical Framework

The theoretical approach of this research integrates several well-established models and criteria in rock mechanics. First, the Rock Quality Designation (RQD) index is used to quantify the degree of fracturing and infer the structural integrity of the rock mass. Based on this, the Geological Strength Index (GSI) is calculated using Barton's empirical formulation that incorporates joint roughness and weathering characteristics. The GSI is then employed within the generalized Hoek–Brown failure criterion, which allows for estimating the peak strength of fractured rock masses. To evaluate rockburst potential, this study applies the brittleness index (UCS/UTS), derived from Griffith's brittle fracture theory, and classifies rockburst risk using the empirical framework proposed by the Canadian Rockburst Program.

For stress analysis, the research applies the Bruno-Kirsch analytical solution, adapted for conditions of thrust fault tectonics, to estimate induced stresses at the excavation boundary. A simplified 3D geomechanical model of the deposit is developed using Kriging-based interpolation of RQD values, facilitating spatial predictions of strength and stability. This integrative framework ensures that both material properties and structural geological conditions are captured, even under data-limited scenarios, such as at the Zhayssan mine.

3. Results

The observed values and their approximation in the model show an increase in mean RQD values with depth: from 60% at 60 m depth to 90% at 540 m depth; this is a very important fact: the quality of the rock mass increases with the lowering of mining operations since the average fracture disturbance of the rock mass decreases. This fact allows us to hope that in the deep horizons of the Zhayssan mine, the growth of rock pressure will be compensated by the growth of quality (strength, stability) of the rock mass.

3.1. Working Strength Forecast

3.1.1. Rock Mass Fracturing Strength Forecast

For strength forecasting, we use the generalized Hooke-Brown criterion (Equation 2). In it, the fracturing of the rock mass is described by the geologic strength index GSI (see section 2.4.3). Based on the analogy with Shatyrkul, we will characterize the roughness of fractures by the index Jr = 3 and the degree of weathering/fracture filling by the index = 1.5. Then, according to Equation 1, we receive $GSI = 35 + 0.5 \cdot RQD$:

RQD =	100	90	80	70	60	50	40	30	20	10
GSI =	85	80	75	70	65	60	55	50	45	40

It is a linear relationship in which the main varying factor is the intensity of fracturing of the RQD rock mass. This factor—the rock mass strength dependence on fracturing intensity—underlies the simplified geomechanical model. This dependence validates the use of RQD-based interpolation for strength modeling in data-scarce environments like Zhayssan. It also allows the model to reflect local heterogeneities, such as weakened metasomatic zones, which cannot be captured using general lithology alone.

Parameters characterizing the fracture properties, roughness Jr and degree of weathering/fracture filling Ja, within the minefield vary slightly. Generally, the calculations use a single mean value of the indicator Jr for the entire deposit. The indicator Ja will likely differ in weathering zones, metasomatism (altered), tectonic faults, and unweathered, fresh rocks. This fact had to be established during the geomechanical rock mass mapping process, which occurred during excavation. The geomechanical model can be brought to a standard state using RMR, GSI, and Q ratings/indices.

Fracturing reduces not only the strength but also the rigidness (deformation modulus) of the rock mass. Figure 20 presents the calculated dependencies of these parameters on the geological strength index GSI and RQD. They were obtained using the Hooke-Brown criterion using the RocLab program. The following properties of the rocks in the samples were used in the calculations: UCS = 87 MPa; mi = 30; Eo = 45 GPa. Rock mass damage by blasting operations was not accounted for (D = 0).

The higher the fracturing intensity, the higher the fracture frequency, the lower the RQD and GSI, and the lower the rock mass strength and deformation modulus. In engineering terms, this underscores that rock mass behavior is not controlled by intact rock strength alone, but significantly by its structural condition. Design decisions such as excavation dimensions, support spacing, and blasting methods must account for localized RQD fluctuations.

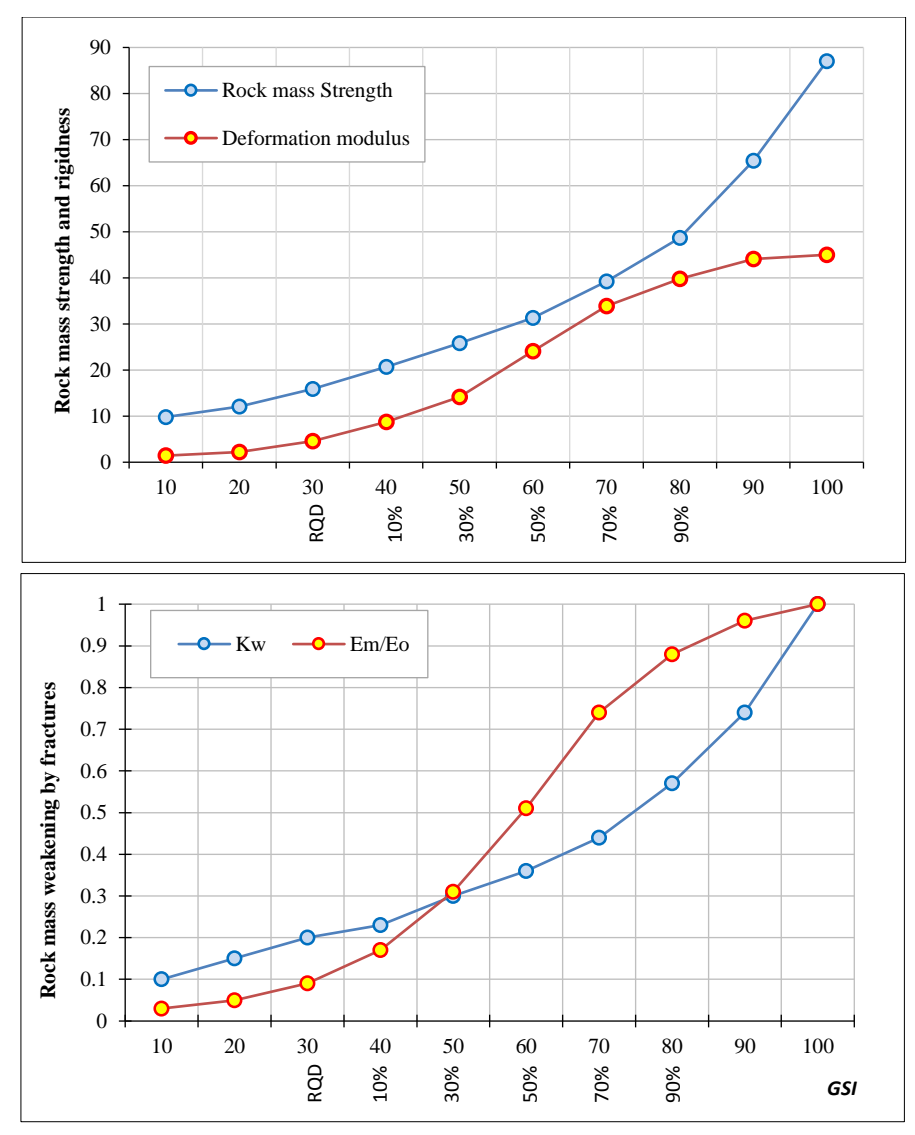


Figure 20. Decrease of the rock mass strength and deformation module due to fracturing

3.1.2. Expected Forms of Working Instability

The miners consider mine workings to be stable if there are no detachments/inrushes/collapses of rock mass from the sides and roof or large displacements of the contour within the entire life of the mine. i.e., the mine workings retain their original (during sinking, ideally - design) dimensions and cross-sectional shape, ensuring the safety of people and performance of process operations (e.g., drilling of cleaning wells, ore loading, and hauling). The main forms of loss of working stability are shown in Figure 21.

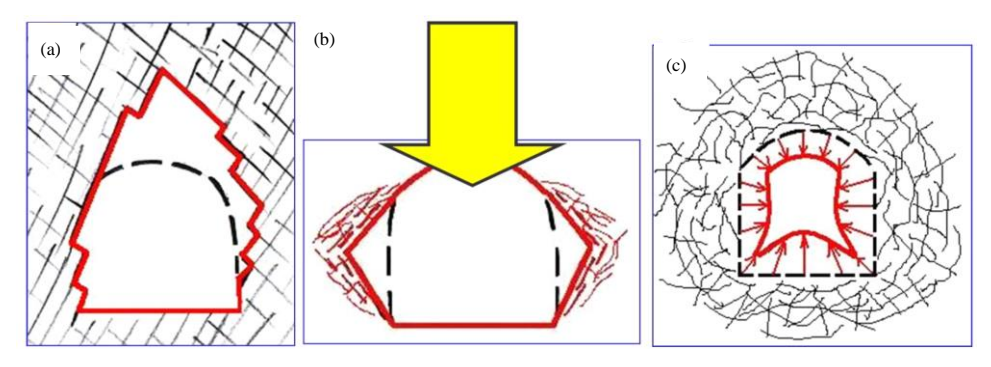


Figure 21. Main Forms of Manifestation of Rock Pressure in Mine Workings: a) Rock block inrushes on the surfaces of rock mass weakening (fractures, faults, polish faults, weak contacts); b) Crushing of rocks by high stresses on the contour of the working (if the maximum stresses act vertically (as in the figure), the sides of the excavation are destroyed; if horizontal tectonic stresses are the maximum ones, in such cases fractures occur in the roof and soil of the excavation); c) Crushing of low-strength rocks at great depth along the entire perimeter of the working, resulting in large displacements of the frame support and reduction of the excavation cross-section (when the support fails, the working cross-section collapses).

According to the experience of the Shatyrkul mine, at the Zhayssan mine, in case of steeply falling occurrence of strong rocks, the rock mass inrushes are the most probable along the steeply falling fractures in the entries along the strike of the rock strata and ore zones (diagram in Figure 21). Rock mass collapse on the Robolt rig in the drill-and-loading entry (DLE) of the 700 m sub-story, north portal No. 6 (Figure 22), which occurred at Shatyrkul mine on 19.05.2021, can be an example.

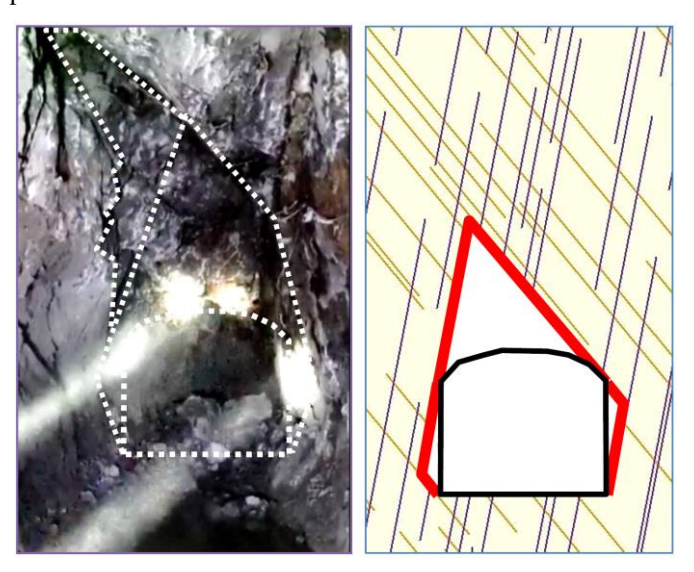


Figure 22. Collapse in DLE of s/s 700 m, North Portal No. 6 at Shatyrkul mine

The collapse occurred in the lined part of the entry together with the anchors. It is seen that, in general, the collapsing zone contour coincides with the steeply dipping fractures (Figure 7). The height of the collapse zone is much greater than the length of the anchors. Rock block inrushes from the entry sides that are not secured are a very characteristic feature. Lateral detachments, at which, as a rule, the responsible persons do not pay attention, cause increases in the width of the working followed by the roof collapsing. Rock detachments from the entry sides have repeatedly led to incidents at Shatyrkul mine.

Also, on 07/04/2020, there was a collapse of the sides and roof of the excavated and lined ventilation entry at horizon 705 m at the length of 21 m with a volume of 109 m³ (Figure 23). The entry was excavated horizontally along the strike of the rock strata and the most developed fractures of lamination 1. According to secant fracture 2, wedge-shaped inrushes from the unlined sides and the lined roof occurred.



Figure 23. Wedge-shaped inrush in the ventilation entry of horizon 705 m at Shatyrkul mine on 07.04.2020

Forms of block inrushes along fractures in the DLE sinking along the rock strata strike are generated by the Unwedge program according to the specified fracture systems and shown in Figure 24.

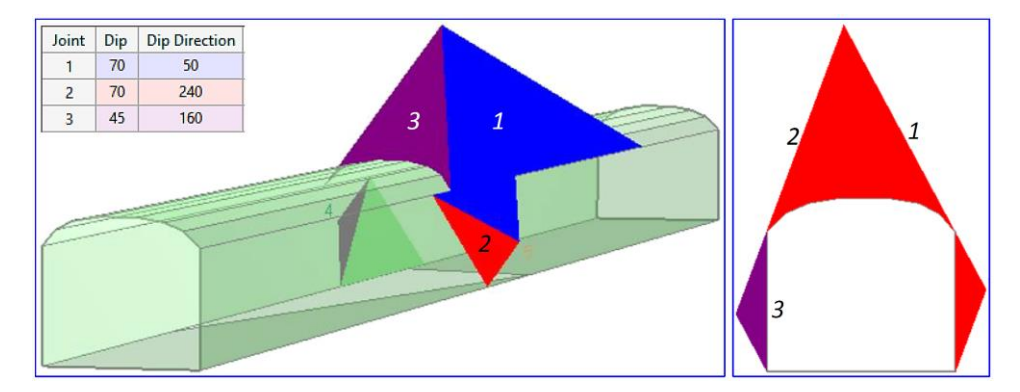
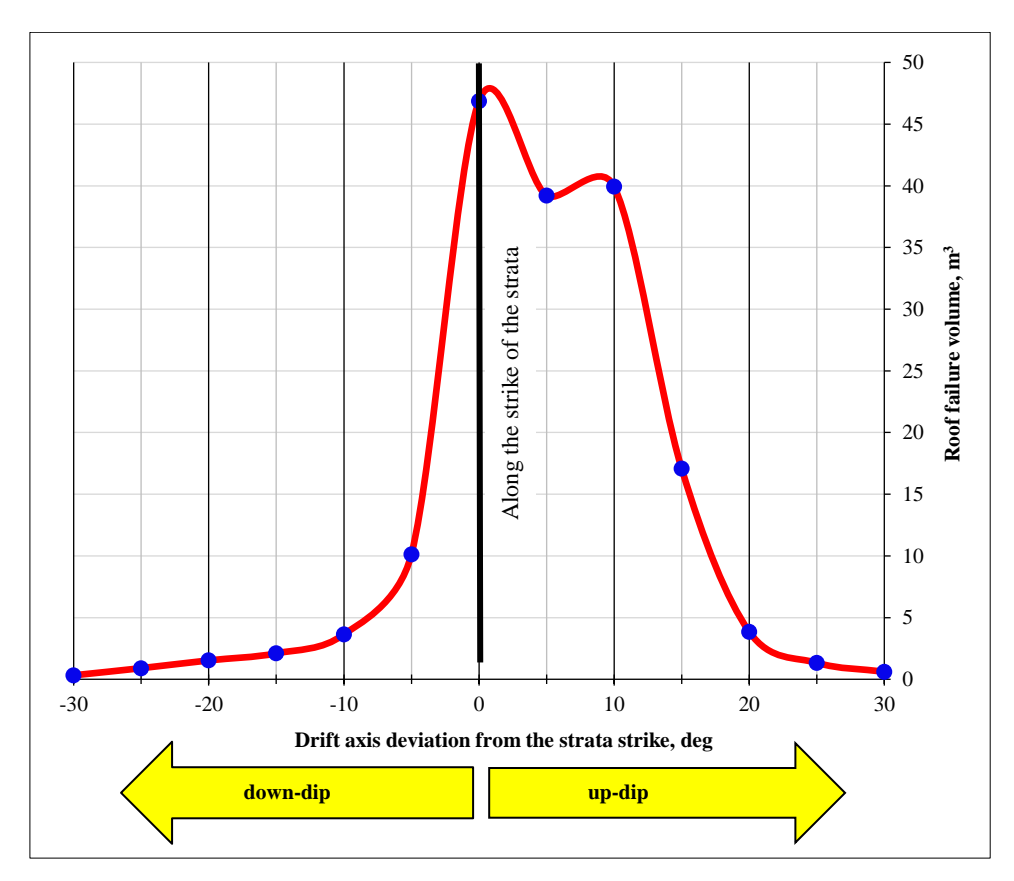


Figure 24. Geometry of possible inrushes in DLE sinking along the strike of ore and host rocks along the fractures: 1 - the most strongly developed system consistent with the dip of the rock strata; 2 - longitudinally secant system with reverse dipping; 3 - cross-sectional system.

The Unwedge program was used to calculate the volumes and heights of inrushes from the DLE roof when the direction of its sinking changes relative to the ore strike and host rocks strata (Figure 25). The results of the kinematic analysis of the inrushes show that:

- The largest volumes of inrushes occur when the entry is excavated along the strike of the rock strata;
- When workings are excavated along the strike of steeply dipping rocks, the height of inrushes from the roof is maximum;
- If the entry axis deviates from the strike of the rock strata, the volume of inrushes and their thickness (maximum height) sharply decreases;
- The larger the cross-sectional area of the working (its dimensions), the greater the volume and height of the inrushes.

Similar processes and phenomena are expected at the Zhayssan mine. Their nature is the kinematic instability of rock blocks formed by systems of steeply dipping fractures. The conditions of their inrushes under their weight are determined by kinematic analysis. The orientation of the fracture systems, the shear resistance of the fractures (cohesion and friction angle), the cross-section, and the working direction must be set.



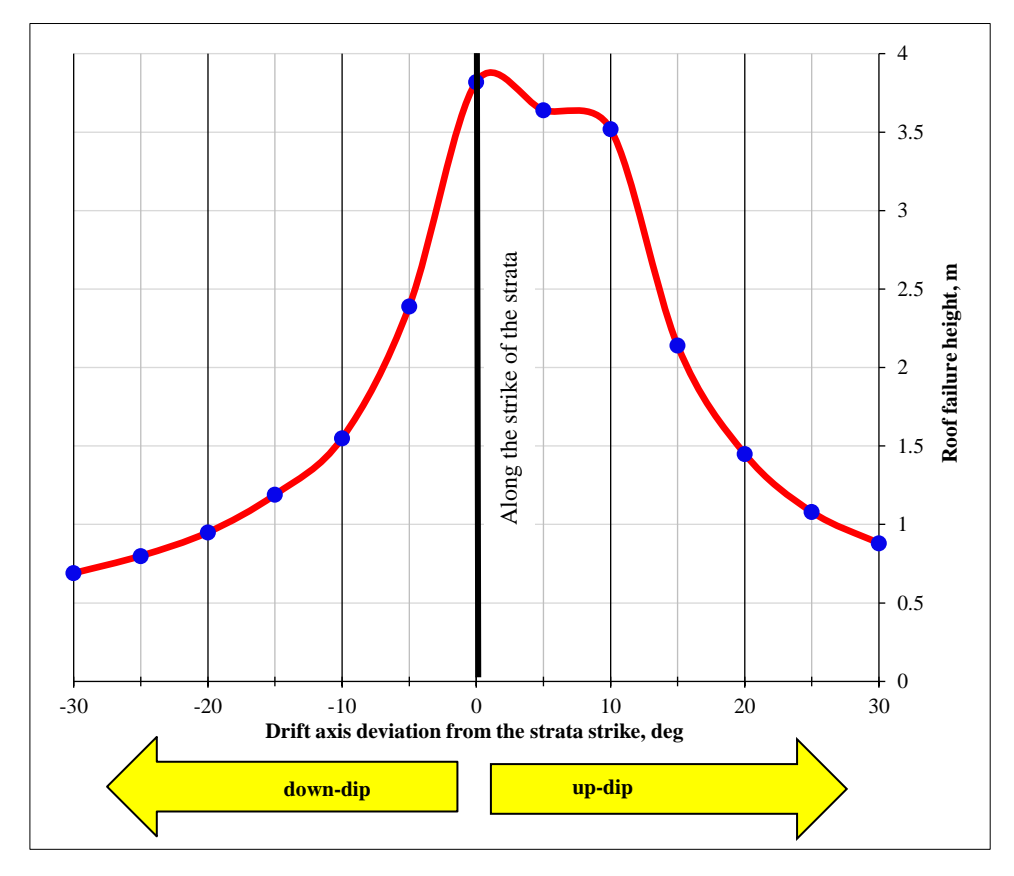


Figure 25. Dependences of volumes (left) and heights (right) of inrushes from the DLE roof on the direction of their sinking concerning the ore strike and thickness of the host rocks

3.2. Rockburst Forecast

The Soviet methodology for assessing the rockburst potential of a rock mass involves two stages: determining the rockburst potential and estimating the stress level sufficient to cause a rockburst [31, 32]. Ores/rocks are recognised as prone to rockbursts if they are elastically deformed (i.e., they accumulate potential energy of elastic deformations) up to destruction and have brittle destruction character (i.e., in the process of destruction, they release accumulated elastic energy quickly at small deformations). All rock formations are elastic. The brittle ones are those in which the recession modulus M is greater than the elastic modulus E.

The elastic modulus E is identified before rock destruction on regular "soft" presses in all ordinary laboratories. To determine the recession modulus M, it is necessary to record the strains in the over-extreme limit state during sample destruction. And this is only possible on "hard" presses, which are much more complex, massive, and expensive than "soft" presses. Obtaining rock recession modulus data for a wide range of deposits has proven problematic due to the limited availability of "hard" tests. Therefore, the brittleness coefficient is used to indirectly assess the rockburst potential of rocks without determining the recession modulus Kbr = UCS/UTS. The criterion of the rockburst potential is Kbr > 10. This criterion is a consequence of Griffiths' brittle fracture criterion [33, 34]. According to it, under tensile stress conditions, the ratio of compression strength UCS and tensile strength UTS shall equal UCS/UTS = 8; under conditions of volume compression - UCS/UTS = 12. The mean figure formulates the condition of brittle fracture of rocks with the brittleness factor UCS/UTS> 10.

The results of long-term, extensive research in Canada on the Canadian Rockburst Program [35] have shown that the Rockburst Severity should be estimated by the Rockburst Potential, which simultaneously considers both the uniaxial compressive strength of rocks UCS and the UCS/UTS brittleness factor. The UCS strength determines the energy accumulated in the rocks when they fracture. The higher the strength, the greater the accumulated energy of elastic deformations, the higher the energy released during fracture, and the stronger the dynamic effect of fracture in the form of inrush and sprinkling of rock mass. The UCS/UTS brittleness factor characterizes the potential (propensity) of rocks to the splitting of thin plates of rocks due to spalling (spalling potential). To determine the rockburst potential of rocks, a diagram is suggested by [35], as shown in Figure 26.

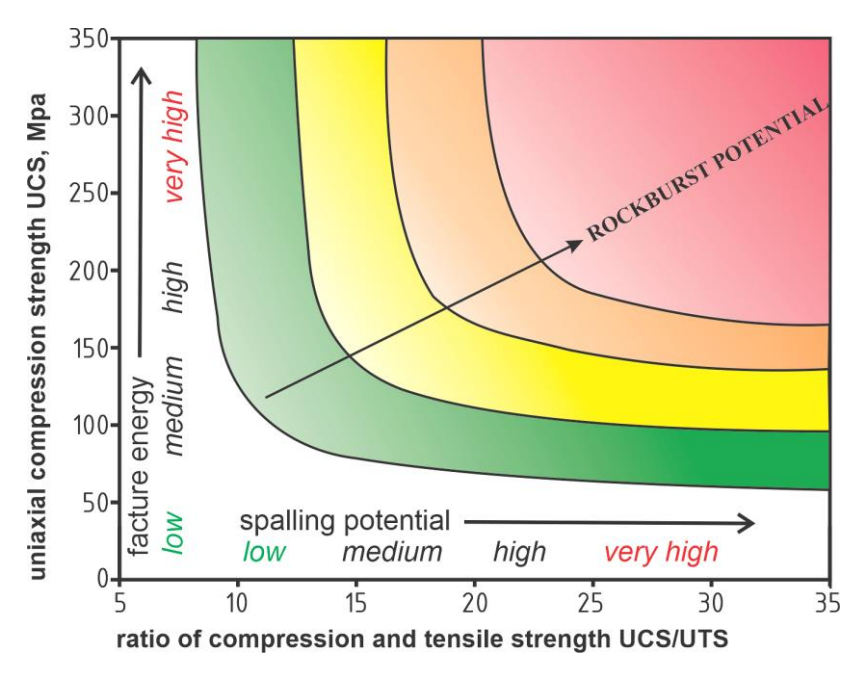


Figure 26. Rockburst potential levels chart (Rockburst potential: LOW, MEDIUM, HIGH, VERY HIGH) depending on the brittleness of UCS/UTS rocks and their uniaxial compressive strength UCS

All available data on rock properties at Zhayssan deposit are plotted on a diagram of rockburst potential levels (Figure 27). Most of the test results (53%) in the diagram fall into region 1 (below the green line), where there is no rockburst potential. In this region, either the rock strength is not high enough to accumulate large potential elastic strain energy by the time of fracture, or the brittleness factor is not high enough for dynamic fracture.

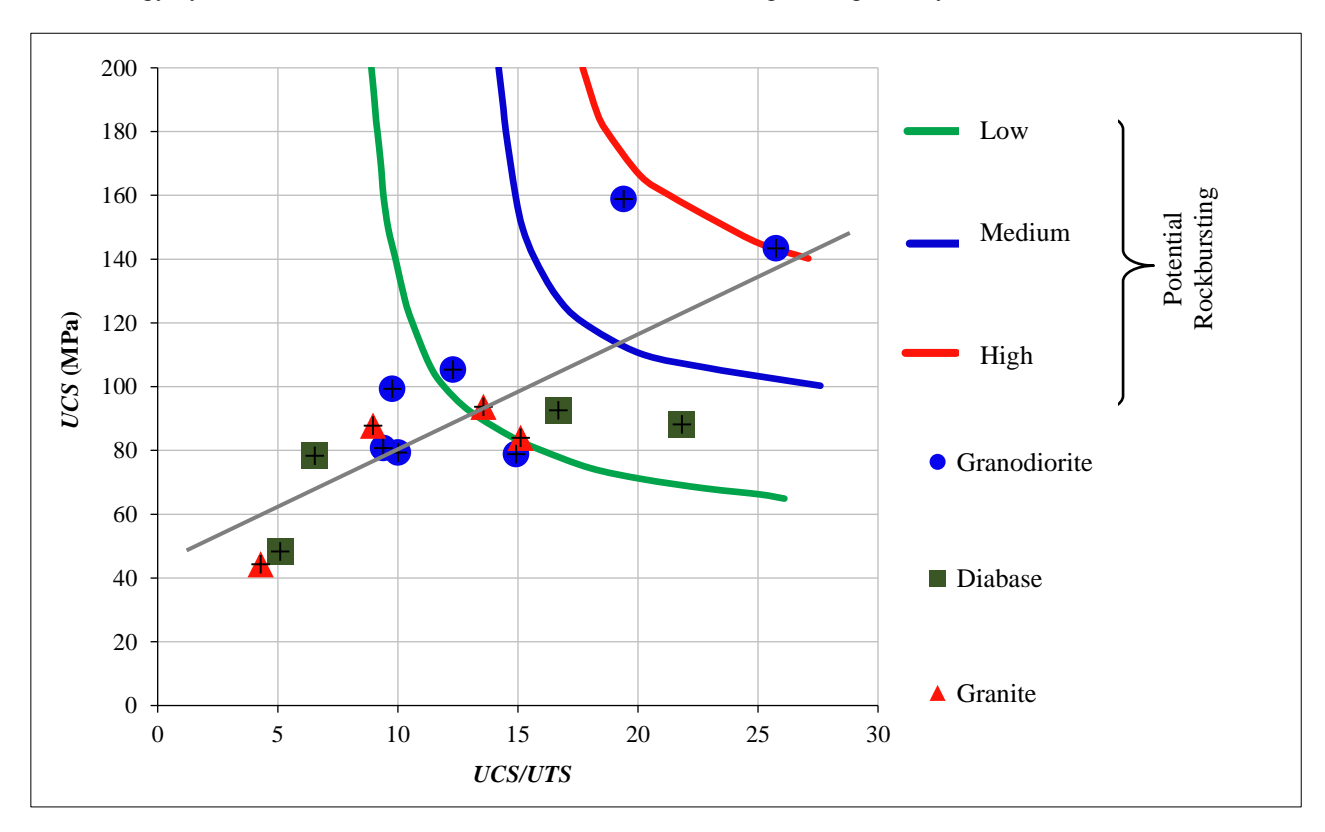


Figure 27. Estimation of rockburst potential of Zhayssan rocks based on the results of laboratory testing of samples; dotted line: trend line $Kbr = 0.14 \cdot UCS$

Area 2 (between the green and blue lines), with a low to medium level of potential, contains 33% of all results. 7% of tests showed medium rockburst potential (area 3 between the blue and red lines). Samples with high rockburst potential (area 4 above the red line) also turned out to be 7%. The distribution of results by rockburst potentials is shown in Figure 28.

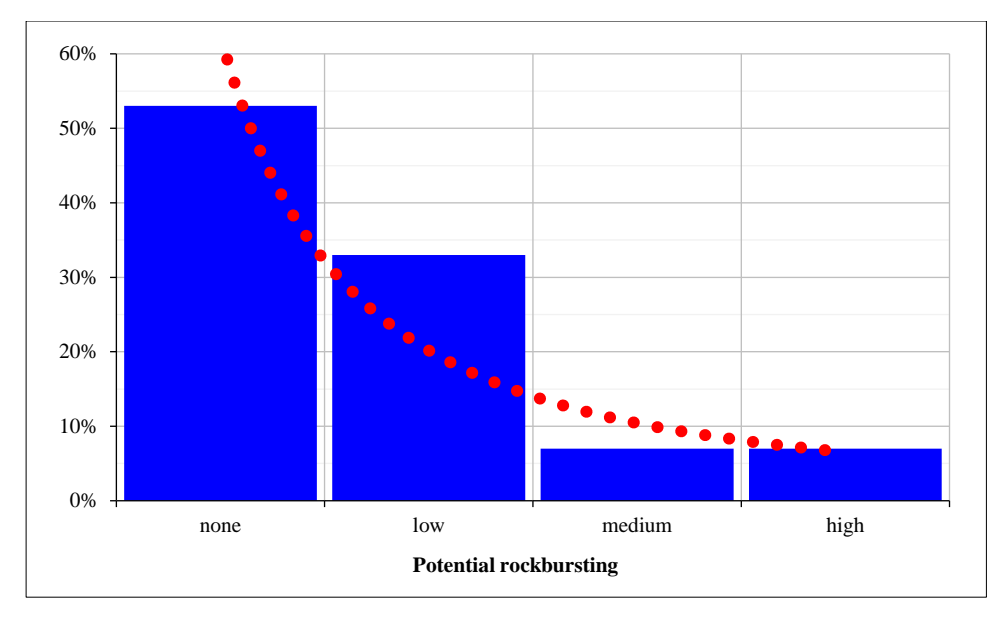


Figure 28. Distribution of Zhayssan rocks volume by Rockburst potential

A linear relationship is observed between the strength of rocks and their brittleness: the greater the strength, the more brittle the rock. With a correlation factor of 0.6, this relationship is as follows: Kbr = 0.14·UCS (Figure 27); this means that at Zhayssan mine, only the strongest and most brittle granitoid varieties, which have not undergone hydrothermal metasomatosis (fresh), are prone to rockbursts. Metasomatites that outline ore zones with the "jacket" are not prone to rockburst due to their reduced strength and brittleness, at which they lose their rockburst potential.

It further suggests that detailed geological mapping to distinguish fresh vs. altered granitoids during excavation is not optional but mandatory. Failure to do so may result in underestimating burst-prone zones or overdesigning support in non-critical areas, affecting both safety and cost-efficiency.

Based on the analytical relationship using UCS = 120–130 MPa, γ = 0.027 MN/m³, and λ_1 = 3, the rockburst-prone depth at the Zhayssan mine is estimated at 390–420 m. For practical use, this value is rounded to a threshold of 400 m, beyond which additional preventive measures are recommended.

This critical depth estimate is not based on empirical observations alone, but rather derives from an analytical formulation using the Bruno–Kirsch equation. Assuming maximum horizontal tectonic stresses ($\sigma_1 = 3\gamma H$), the onset of rockburst is projected to occur when the induced stress at excavation boundaries exceeds 70% of UCS [36]. Given the observed UCS range of 120–130 MPa for fresh granitoids and a unit weight $\gamma = 0.027$ MN/m³, this corresponds to a rockburst threshold depth of approximately 390–420 m. The value of 400 m is therefore a theoretically supported boundary, validated against mechanical strength and stress interaction criteria [37-39].

This finding is critical for safety planning, as it sets a depth threshold for the implementation of preventive rockburst measures. From this depth onward, enhanced monitoring (e.g., microseismic arrays), flexible support systems, and stress-relief techniques become essential to mitigate dynamic hazards.

Overall, the results provide a depth-specific view of geomechanical hazards at Zhayssan. They demonstrate that structural weakening in the upper horizons and stress-driven risks at depth form a dual challenge. The applied modeling framework allows the identification of transition zones and enables targeted support strategies that differ across the vertical extent of the mine.

4. Discussion

The study of rock mass quality at the Zhayssan deposit demonstrates a regular increase in rock mass stability with depth, which is consistent with previously published data of other authors on the effect of increasing rock pressure on improving the mechanical properties of rocks [1, 2]. In particular, the increase in the strength and stability of the rock mass as depth increases is confirmed by the detected increase in the average RQD value from 60% at the upper horizons to 90% at depths greater than 500 m; this is consistent with the findings of Zhang et al. that increasing mining depth promotes rock mass stabilization by rocks transitioning from brittle to ductile characteristics [3].

Nevertheless, the results show that significant geomechanical risks accompany the predicted positive trends in the mechanical properties of the rock mass. The problems associated with the presence of metasomatic alteration zones, where rock strength is significantly reduced, are emphasised, which is confirmed by similar observations at the nearby Shatyrkul deposit. This heterogeneity of the rock mass can lead to significant discrepancies between the forecasted and actual stability of mine workings, especially in metasomatite zones. Moreover, the altered zones exhibit enhanced

water sensitivity, as observed in laboratory tests under saturated conditions. While this study did not include direct hydrogeological modeling, the identified weakening effect of water interaction suggests a significant influence of groundwater on mechanical stability at depth, which warrants integration into future multi-physics simulations.

A critical discrepancy with the forecasts from previous studies was revealed in the context of the rockburst potential of the rock mass. According to Cai and Kaiser [35], if the rock mass's strength at great depths accumulates significant elastic energy at the Zhayssan deposit, this effect is manifested unevenly and predominantly in fresh granitoids. The experimental data obtained indicate that there is only a limited share of rocks (about 7%) with high rockburst potential; this significantly limits the possibility of applying generalized forecast models, such as the proposed Canadian methodology, without considering specific local geological conditions.

The study's limitations are related to the limited amount of laboratory testing, the absence of instrumental stress monitoring, and the insufficient data for a comprehensive 3D model. The absence of full-scale stress measurements for the Zhayssan deposit should also be considered: these measurements have been replaced by equivalents from the neighboring Shatyrkul mine; this limits the reliability of the conclusions drawn about the stress state and rockburst potential.

The results of this study are consistent with prior research indicating that deeper mining levels may exhibit higher rock mass quality due to stress-induced compaction and reduced fracturing. For instance, Zhang et al. [3] and Zhou et al. [10] observed that increasing depth can lead to a transition from brittle to ductile rock behavior, which contributes to enhanced rock stability. Similar depth-related strengthening trends were confirmed at Zhayssan.

However, the present study diverges from previous works in its treatment of metasomatic alterations. Unlike earlier models that assume uniform lithological behavior with depth, our findings emphasize that metasomatically altered zones retain low strength and brittleness, even at significant depths — a conclusion supported by comparison with Shatyrkul mine data. This highlights a limitation in existing generalized depth-based prediction models, as proposed by Sun et al. [8] and Wang et al. [9], which do not account for local alteration zones.

Furthermore, while studies like those by Rojas Perez et al. [14] found consistent rockburst initiation depths in hard rock mines around 1200–1500 m, our case shows that high tectonic stresses under thrust faulting conditions can cause rockburst potential as shallow as 400 m. This discrepancy underscores the importance of local stress regimes, which are often overlooked in global predictive frameworks.

In summary, the present study confirms some established patterns (e.g., depth-related quality improvement), but also identifies critical exceptions linked to geological heterogeneity and tectonic stress orientation, which require mine-specific calibration of forecasting methods.

In conclusion, while this study confirms that rock mass quality generally improves with depth, it also highlights critical exceptions linked to metasomatic alteration and stress anisotropy. Future research should focus on expanding mechanical testing, hydrogeological monitoring, and in situ stress measurements to refine depth-specific forecasting and improve risk management strategies.

5. Conclusion

This study investigated the quality of the rock mass and the rockburst risk variation with depth at the Zhayssan mine in southeastern Kazakhstan. A multi-step methodology combining laboratory testing, field analogs, and geomechanical modeling was applied to overcome limitations in in situ data. The simplified geomechanical model was based on the RQD index, which served as the key parameter for assessing rock mass integrity and strength distribution with depth.

The results demonstrated that the average RQD increases with depth, indicating a decrease in fracturing and an improvement in rock mass quality – from 60% at shallow levels to around 90% at greater depths (>500 m). This trend was accompanied by a corresponding increase in the geological strength index (GSI) and strength parameters of the rock mass. However, despite improved structural integrity at depth, the rockburst hazard remains critical, particularly due to the dominance of horizontal tectonic stresses under thrust faulting regimes. Using the UCS/UTS brittleness index and the Canadian rockburst potential framework, the rockburst threshold depth was estimated at approximately 400 m. Notably, metasomatically altered granitoids near ore zones showed significantly reduced strength and rockburst potential, while fresh brittle granitoids at depth remained highly prone to dynamic failure.

The findings confirm the need for depth-sensitive and geology-specific approaches to mine design and hazard assessment. Unlike general models that focus on depth alone, this study emphasizes the combined effects of structural heterogeneity and tectonic stress fields. Future work should expand laboratory testing, introduce microseismic monitoring, and enhance the calibration of numerical models. The integrative approach proposed here provides a practical framework for geomechanical risk forecasting at sites with limited initial data, and it may serve as a reference for similar hard-rock mining operations worldwide.

6. Declarations

6.1. Author Contributions

Conceptualization, D.K.T. and G.S.; methodology, M.Z.B.; validation, D.T.I., M.A.Z., and Z.A.; formal analysis, M.Z.B.; investigation, M.Z.B.; resources, M.A.Z.; data curation, Z.A.; writing—original draft preparation, D.K.T.; writing—review and editing, G.S. and D.T.I.; visualization, M.A.Z.; supervision, G.S.; project administration, D.K.T.; funding acquisition, D.K.T. All authors have read and agreed to the published version of the manuscript.

6.2. Data Availability Statement

The data presented in this study are available on request from the corresponding.

6.3. Funding

This research is funded by the Committee of Science of the Ministry of Science and Higher Education of the Republic of Kazakhstan (grant No. AP19677938).

6.4. Acknowledgements

The researchers wish to express their sincere gratitude to the Committee of Science of the Ministry of Science and Higher Education of the Republic of Kazakhstan, as well as to the Abylkas Saginov Karaganda Technical University, represented by the Department of Geology and Exploration of Mineral Deposits, for the financial support and the material and technical base provided. Special thanks are expressed to the experts whose substantive recommendations significantly contributed to improving the content and overall quality of this study. The authors also thank Kazakhmys Corporation LLP for assistance in conducting laboratory tests, and Elsevier for assistance in editing the English text.

6.5. Conflicts of Interest

The authors declare no conflict of interest.

7. References

- [1] Li, S., Wang, L., Ren, Q., Zhu, C., Liu, H., Liu, H., & Chen, L. (2022). A Study on the Influence of Mining Depth on the Stress Distribution Characteristics of Stope Surrounding Rock. Geofluids, 2022, 1–12. doi:10.1155/2022/4178554.
- [2] Wu, H., Wang, X., Yu, W., Wang, W., Zhang, Z., & Peng, G. (2020). Analysis of influence law of burial depth on surrounding rock deformation of roadway. Advances in Civil Engineering, 2020, 8870800. doi:10.1155/2020/8870800.
- [3] Zhang, C., Ye, D., Yang, P., Wu, S., & Wang, C. (2020). Study on impact tendency of coal and rock mass based on different stress paths. Advances in Civil Engineering, 2020, 8883537. doi:10.1155/2020/8883537.
- [4] Cheng, L., Zhang, Y., Ji, M., Cui, M., Zhang, K., & Zhang, M. (2015). Theoretical Calculation and Analysis on the Composite Rock-Bolt Bearing Structure in Burst-Prone Ground. Mathematical Problems in Engineering, 2015, 1–6. doi:10.1155/2015/434567.
- [5] Kang, H. (2014). Support technologies for deep and complex roadways in underground coal mines: a review. International Journal of Coal Science & Technology, 1(3), 261–277. doi:10.1007/s40789-014-0043-0.
- [6] Mussin, A., Kydrashov, A., Asanova, Z., Abdrakhman, Y., & Ivadilinova, D. (2024). Ore dilution control when mining low-thickness ore bodies using a system of sublevel drifts. Mining of Mineral Deposits, 18(2), 18–27. doi:10.33271/mining18.02.018.
- [7] Ghazdali, O., Moustadraf, J., Tagma, T., Alabjah, B., & Amraoui, F. (2021). Study and evaluation of the stability of underground mining method used in shallow-dip vein deposits hosted in poor quality rock. Mining of Mineral Deposits, 15(3), 31–38. doi:10.33271/MINING15.03.031.
- [8] Sun, L., Hu, N., Ye, Y., Tan, W., Wu, M., Wang, X., & Huang, Z. (2022). Ensemble stacking rockburst prediction model based on Yeo–Johnson, K-means SMOTE, and optimal rockburst feature dimension determination. Scientific Reports, 12(1), 15352. doi:10.1038/s41598-022-19669-5.
- [9] Wang, H., Li, Z., Song, D., He, X., Sobolev, A., & Khan, M. (2021). An intelligent rockburst prediction model based on scorecard methodology. Minerals, 11(11), 1294. doi:10.3390/min11111294.
- [10] Zhu, Q., Zhao, X., & Westman, E. (2021). Review of the Evolution of Mining-Induced Stress and the Failure Characteristics of Surrounding Rock Based on Microseismic Tomography. Shock and Vibration, 2154857. doi:10.1155/2021/2154857.
- [11] Zeitinova, S., Imashev, A., Bakhtybayev, N., Matayev, A., Mussin, A., & Yeskenova, G. (2024). Numerical Modeling the Rock Mass Stress-Strain State Near Vertical Excavations in Combined Mining. Civil Engineering Journal (Iran), 10(9), 2919–2934. doi:10.28991/CEJ-2024-010-09-010.

- [12] Zholmagambetov, N., Khalikova, E., Demin, V., Balabas, A., Abdrashev, R., & Suiintayeva, S. (2023). Ensuring a safe geomechanical state of the rock mass surrounding the mine workings in the Karaganda coal basin, Kazakhstan. Mining of Mineral Deposits, 17(1), 74–83. doi:10.33271/mining17.01.074.
- [13] Abdiev, A. R., Wang, J., Mambetova, R. S., Abdiev, A. A., & Abdiev, A. S. (2025). Geomechanical assessment of stress-strain conditions in structurally heterogeneous rock masses of Kyrgyzstan. Engineering Journal of Satbayev University, 147(2), 31–39. doi:10.51301/ejsu.2025.i2.05.
- [14] Rojas Perez, C., Wei, W., Gilvesy, A., Borysenko, F.-J., & Mitri, H. (2024). Rockburst assessment and control: a case study of a deep sill pillar recovery. Deep Mining 2024: Proceedings of the 10th International Conference on Deep and High Stress Mining, Australian Centre for Geomechanics, Perth, 659–672. doi:10.36487/acg_repo/2465_40.
- [15] Cortés, N., Hekmatnejad, A., Pan, P., Mohtarami, E., Pena, A., Taheri, A., & González, C. (2024). Empirical approaches for rock burst prediction: A comprehensive review and application to the new level of El Teniente Mine, Chile. Heliyon, 10(5), e26515. doi:10.1016/j.heliyon.2024.e26515.
- [16] Heidbach, O., Barth, A., Müller, B., Reinecker, J., Stephansson, O., Tingay, M., & Zang, A. (2016). WSM quality ranking scheme, database description and analysis guidelines for stress indicator. WSM Technical Report 16-01, World Stress Map Project, Potsdam, Germany.
- [17] Kayal, J. (2008). Dynamics of Faulting and Fault Plane Solution. In: Micro-earthquake Seismology and Seismotectonics of South Asia. Springer, Dordrecht, Netherlands. doi:10.1007/978-1-4020-8180-4_4.
- [18] Röckel, L., Ahlers, S., Müller, B., Reiter, K., Heidbach, O., Henk, A., Hergert, T., & Schilling, F. (2022). The analysis of slip tendency of major tectonic faults in Germany. Solid Earth, 13(6), 1087–1105. doi:10.5194/se-13-1087-2022.
- [19] Abdiev, A. R., Mambetova, R. S., & Mambetov, S. A. (2017). Geomechanical assessment of Tyan-Shan's mountains structures for effi cient mining and mine construction. Gornyi Zhurnal, 4(4), 23–28. doi:10.17580/gzh.2017.04.04.
- [20] Kazakhmys (2020). Mining plan for the development of Zhomart deposit. Kazakhmys Corporation LLP Head Design Institute. Astana, Kazakhstan.
- [21] Takhanov, D., Zhienbayev, A., & Zharaspaev, M. (2024). Determining the parameters for the overlying stratum caving zones during re-peated mining of pillars. Mining of Mineral Deposits, 18(2), 93–103. doi:10.33271/mining18.02.093.
- [22] Zhienbayev, A., Balpanova, M., Asanova, Z., Zharaspaev, M., Nurkasyn, R., & Zhakupov, B. (2023). Analysis of the roof span stability in terms of room-and-pillar system of ore deposit mining. Mining of Mineral Deposits, 17(1), 129–137. doi:10.33271/mining17.01.129.
- [23] Zhienbayev, A., Takhanov, D., Zharaspaev, M., Kuttybayev, A., Rakhmetov, B., & Ivadilinova, D. (2025). Identifying rational locations for field mine workings in the zone influenced by mined-out space during repeated mining of pillars. Mining of Mineral Deposits, 19(1), 1–12. doi:10.33271/mining19.01.001.
- [24] Somodi, G., Bar, N., Kovács, L., Arrieta, M., Török, Á., & Vásárhelyi, B. (2021). Study of rock mass rating (RMR) and Geological Strength index (GSI) correlations in granite, siltstone, sandstone and quartzite rock masses. Applied Sciences, 11(8), 3351. doi:10.3390/app11083351.
- [25] Ahrami, O., Javaheri Koupaei, H., & Ahangari, K. (2024). Determination of deformation modulus and characterization of anisotropic behavior of blocky rock masses. Mining Science and Technology (Russian Federation), 9(2), 116–133. doi:10.17073/2500-0632-2023-08-143.
- [26] Kulbayev, B., Lapin, V., Shakhnovich, A., Shokbarov, Y., Tuleyev, T., Aldakhov, S., Aldakhov, Y., & Ali, A. (2024). Strength and Deformability of Structural Steel for Use in Construction. Civil Engineering Journal (Iran), 10(3), 796–807. doi:10.28991/CEJ-2024-010-03-09.
- [27] Barton, N. (2002). Some new Q-value correlations to assist in site characterisation and tunnel design. International Journal of Rock Mechanics and Mining Sciences, 39(2), 185–216. doi:10.1016/S1365-1609(02)00011-4.
- [28] Lin, F., Luan, H., Zeng, Y., & Zhong, Z. (2017). Some New Correlations of Q-Value with Rock Mechanics Parameters in Underground Oil Storage Caverns. Civil Engineering Journal, 3(8), 537–546. doi:10.28991/cej-2017-00000111.
- [29] Hoek, E., & Brown, E. T. (2019). The Hoek–Brown failure criterion and GSI 2018 edition. Journal of Rock Mechanics and Geotechnical Engineering, 11(3), 445–463. doi:10.1016/j.jrmge.2018.08.001.
- [30] Liu, Z., Guo, Y., Du, S., Wu, G., & Pan, M. (2017). Research on calibrating rock mechanical parameters with a statistical method. PLoS ONE, 12(5), 0176215. doi:10.1371/journal.pone.0176215.
- [31] Petukhov, I. M., Linkov, A. M., Sidorov, V. S., & Feldman, I.A. (1976). Theory of Protective Layers. Nedra, Moscow, Russia. (In Russian).
- [32] Petukhov, I. M., & Linkov, A. M. (1983). Mechanics of rock bursts and outbursts. Nedra, Moscow, Russia. (In Russian).

- [33] Lajtai, E. Z. (1971). A theoretical and experimental evaluation of the Griffith theory of brittle fracture. Tectonophysics, 11(2), 129–156. doi:10.1016/0040-1951(71)90060-6.
- [34] Alessi, R., & Ulloa, J. (2023). Endowing Griffith's fracture theory with the ability to describe fatigue cracks. Engineering Fracture Mechanics, 281. doi:10.1016/j.engfracmech.2023.109048.
- [35] Cai, M., & Kaiser, P. K. (2018). Rockburst Support Reference Book Volume I: Rockburst phenomenon and support characteristics. Mining Innovation, Laurentian University (MIRARCO), Sudbury, Canada.
- [36] GOV.KZ (2014). Rules for ensuring industrial safety for hazardous production facilities engaged in mining and geological exploration. Order of the Minister of Investment and Development of the Republic of Kazakhstan dated December 30, 2014 No. 352.
- [37] Makarov, A. B. (2006). Practical geomechanics. Mining book, Moscow, Russia. (In Russian).
- [38] Kirsch, E. G. (1898). The Theory of Elasticity and the Requirements of Strength of Materials. Zeitshrift des Vereines deutscher Ingenieure, 42, 797-807. (In German).
- [39] Rezini, D., Khaldi, A., & Rahmani, Y. (2015). On the Boundary Value Kirsch's Problem. Journal of Mechanics, 32(1), 1–10. doi:10.1017/jmech.2015.93.